Wake Vortex Separation Standards: Analysis Methods

Research and Special Programs Administration
John A. Volpe
National Transportation Systems Center
Cambridge, MA 02142-1093

Final Report
May 1997

19970714 067

U. S. Department of Transportation

Federal Aviation Administration

REPORT DOCUMENTATION PAGE

Form Approved
OMB No. 0704-0188

Public reporting burden for this collection of information is estimated to average 1 hour per response, including the time for reviewing instructions, searching existing data sources, gathering and maintaining the data needed, and completing and reviewing the collection of information. Send comments regarding this burden estimate or any other aspect of this collection of information, including suggestions for reducing this burden, to Washington Headquarters Services, Directorate for Information Operations and Reports, 1215 Jefferson Davis Highway, Suite 1204, Arlington, VA 22202-4302, and to the Office of Management and Budget, Paperwork Reduction Project (0704-0188), Washington, DC 20503.

1. AGENCY USE ONLY (Leave blank)	2. REPORT DATE May 1997	3. REPORT TYPE AND DATES COVERED Final Report January 1997 – March 1997

4. TITLE AND SUBTITLE Wake Vortex Separation Standards: Analysis Methods	5. FUNDING NUMBERS FA727/A7072 DTRS-57-93-D-00070
6. AUTHOR(S) David Burnham[*] and James Hallock	

7. PERFORMING ORGANIZATION NAME(S) AND ADDRESS(ES) U.S. Department of Transportation Research and Special Programs Administration John A. Volpe National Transportation Systems Center Cambridge, MA 02142-1093	8. PERFORMING ORGANIZATION REPORT NUMBER DOT-VNTSC-FAA-97-4

9. SPONSORING/MONITORING AGENCY NAME(S) AND ADDRESS(ES) U.S. Department of Transportation Federal Aviation Administration Office of Communications, Navigation and Surveillance Systems 800 Independence Ave., S.W. Washington, DC 20591	10. SPONSORING/MONITORING AGENCY REPORT NUMBER DOT/FAA/ND-97-4

11. SUPPLEMENTARY NOTES
[*]Scientific & Engineering Solutions, Inc.
Orleans, MA

12a. DISTRIBUTION/AVAILABILITY STATEMENT This document is available to the public through the National Technical Information Service, Springfield, VA 22161	12b. DISTRIBUTION CODE

13. ABSTRACT (Maximum 200 words)
Wake vortex separation standards are used to prevent hazardous wake vortex encounters. A "safe" separation model can be used to assess the safety of proposed changes in the standards. A safe separation model can be derived from an encounter hazard model and a vortex decay model. This report presents subsequent developments and applications of such a model which was first developed in the early 1980s. A static encounter hazard model is coupled with a decay model based on sodar measurements of vortex decay. The separation standards and procedures used from 1976 to 1994 are assumed to be safe based on the absence of IFR accidents. Various versions of the model are used to assess how aircraft should be classified and to evaluate the safety of a possible four-class aircraft separation system. Recommendations are made for ways of improving the safe separation models.

14. SUBJECT TERMS wake vortices, wake vortex encounter, separation standards, vortex decay model, vortex hazard model, vortex strength	15. NUMBER OF PAGES 88
	16. PRICE CODE

17. SECURITY CLASSIFICATION OF REPORT Unclassified	18. SECURITY CLASSIFICATION OF THIS PAGE Unclassified	19. SECURITY CLASSIFICATION OF ABSTRACT Unclassified	20. LIMITATION OF ABSTRACT

NSN 7540-01-280-5500

Standard Form 298 (Rev. 2-89)
Prescribed by ANSI Std. 239-18
298-102

PREFACE

The work reported here reflects the efforts of the John A. Volpe National Transportation Systems Center, (Volpe Center) during many different periods of the Federal Aviation Administration (FAA) Wake Vortex Program:

1. The original separation model for landing aircraft was developed in the late 1970s and was first used to address the possible classification of Heavy DC-8 and B-707 aircraft as Large. It was subsequently applied to a number of additional cases in the 1980s and 1990s.

2. In the 1980s, a different model was developed for aircraft classification, for both takeoff and landing.

3. In the 1990s, a new vortex strength parameter was developed to make hazard results insensitive to measurements of the vortex core which (a) are inaccurate for all vortex sensors and (b) are irrelevant to vortex encounter modeling since, for a worst-case encounter, the core will be occupied by the encountering aircraft's fuselage, not its wing. A new, alternative form of the separation model was based on the new strength parameter.

These separation/classification models made use of wake-vortex decay data collected in 1976-1977 (landing) and 1980 (takeoff) at Chicago's O'Hare Airport.

In 1994, in response to two accidents involving business jets following B-757 aircraft, the FAA temporarily increased the required spacings behind the B-757 by one mile. In 1995, the FAA asked an industry team to provide recommendations on aircraft classifications and separations. The new or alternative separation model results presented in this report were provided to this team. The team report was submitted to the FAA on June 13, 1995, with a number of recommendations, including revised three- and four-class separation systems. The FAA Wake Vortex Program Manager, George C. (Cliff) Hay, asked the Volpe Center to provide a detailed analysis of one version of the recommended four-class system. The analysis is presented in this report. In August 1996, the FAA finalized a new separation/classification system that retained special increased separations for the B-757 and increased the weight breakpoint between the Small and Large classes. None of the work presented in this report reflects operational experience under the recent 1994-1996 changes in separation standards. Instead, the analysis is based on the two decades of operational experience with the separation standards in use before 1994.

Many presentations and conversations at the October 1991 International Wake Vortex Symposium contributed to the concepts explored in this report. Tom Talbot of System Technology Corporation assisted with many of the early calculations. George Greene of the NASA Langley Research Center and Edward Spitzer of the Volpe Center helped define the scope of this work and gave many helpful suggestions.

METRIC/ENGLISH CONVERSION FACTORS

ENGLISH TO METRIC

LENGTH (APPROXIMATE)

1 inch (in) = 2.5 centimeters (cm)
1 foot (ft) = 30 centimeters (cm)
1 yard (yd) = 0.9 meter (m)
1 mile (mi) = 1.6 kilometers (km)

AREA (APPROXIMATE)

1 square inch (sq in, in²) = 6.5 square centimeters (cm²)
1 square foot (sq ft, ft²) = 0.09 square meter (m²)
1 square yard (sq yd, yd²) = 0.8 square meter (m²)
1 square mile (sq mi, mi²) = 2.6 square kilometers (km²)
1 acre = 0.4 hectare (ha) = 4,000 square meters (m²)

MASS - WEIGHT (APPROXIMATE)

1 ounce (oz) = 28 grams (gm)
1 pound (lb) = .45 kilogram (kg)
1 short ton = 2,000 pounds (lb) = 0.9 tonne (t)

VOLUME (APPROXIMATE)

1 teaspoon (tsp) = 5 milliliters (ml)
1 tablespoon (tbsp) = 15 milliliters (ml)
1 fluid ounce (fl oz) = 30 milliliters (ml)
1 cup (c) = 0.24 liter (l)
1 pint (pt) = 0.47 liter (l)
1 quart (qt) = 0.96 liter (l)
1 gallon (gal) = 3.8 liters (l)
1 cubic foot (cu ft, ft³) = 0.03 cubic meter (m³)
1 cubic yard (cu yd, yd³) = 0.76 cubic meter (m³)

TEMPERATURE (EXACT)

$°C = 5/9(°F - 32)$

METRIC TO ENGLISH

LENGTH (APPROXIMATE)

1 millimeter (mm) = 0.04 inch (in)
1 centimeter (cm) = 0.4 inch (in)
1 meter (m) = 3.3 feet (ft)
1 meter (m) = 1.1 yards (yd)
1 kilometer (km) = 0.6 mile (mi)

AREA (APPROXIMATE)

1 square centimeter (cm²) = 0.16 square inch (sq in, in²)
1 square meter (m²) = 1.2 square yards (sq yd, yd²)
1 square kilometer (km²) = 0.4 square mile (sq mi, mi²)
10,000 square meters (m²) = 1 hectare (ha) = 2.5 acres

MASS - WEIGHT (APPROXIMATE)

1 gram (gm) = 0.036 ounce (oz)
1 kilogram (kg) = 2.2 pounds (lb)
1 tonne (t) = 1,000 kilograms (kg) = 1.1 short tons

VOLUME (APPROXIMATE)

1 milliliter (ml) = 0.03 fluid ounce (fl oz)
1 liter (l) = 2.1 pints (pt)
1 liter (l) = 1.06 quarts (qt)
1 liter (l) = 0.26 gallon (gal)
1 cubic meter (m³) = 36 cubic feet (cu ft, ft³)
1 cubic meter (m³) = 1.3 cubic yards (cu yd, yd³)

TEMPERATURE (EXACT)

$°F = 9/5(°C) + 32$

QUICK INCH-CENTIMETER LENGTH CONVERSION

INCHES	0	1	2	3	4	5

CENTIMETERS	0	1	2	3	4	5	6	7	8	9	10	11	12	13

QUICK FAHRENHEIT-CELSIUS TEMPERATURE CONVERSION

°F	-40°	-22°	-4°	14°	32°	50°	68°	86°	104°	122°	140°	158°	176°	194°	212°
°C	-40°	-30°	-20°	-10°	0°	10°	20°	30°	40°	50°	60°	70°	80°	90°	100°

For more exact and or other conversion factors, see NIST Miscellaneous Publication 286, Units of Weights and Measures. Price $2.50. SD Catalog No. C13 10286.

Updated 8/1/96

TABLE OF CONTENTS

TABLE OF CONTENTS (Cont.)

TABLE OF CONTENTS (Cont.)

LIST OF ILLUSTRATIONS

LIST OF ACRONYMS AND TERMS

A	Actual separation distance
ATC	Air Traffic Control
b	Wingspan of vortex encountering (following) aircraft
B	Wingspan of vortex generating (leading) aircraft
CTAS	Center Tracon Automation System
C_{lv}	Vortex-induced torque coefficient
D	Safe separation distance
d_H	Hazard distance
e	Engine-placement term in decay time equation
E	Engine configuration (E =0 except E = 1 for aircraft with two wing-mounted engines)
EER	Equal Encounter Rate
f	Fraction of maximum roll control that pilot can effectively use in countering the vortex-induced roll
FAA	Federal Aviation Administration
FY	Fiscal Year
g	Gravitational acceleration (9.8 m/sec^2)
G	Constant in power-law safe separation distance equation
H	Heavy class
IFR	Instrument Flight Rules
K	Non-dimensional wing-loading constant
lb	Pound
L	Large class
LDV	Laser Doppler Velocimeter
m	Safe separation distance power law for generating aircraft wingspan
M	Medium class
MAVSS	Monostatic Acoustic Vortex Sensing System
MCGTOW	Maximum Certificated Gross Take Off Weight
n	Power in decay law
nm	Nautical Mile
OAG	Official Airline Guide
p	Roll rate (radians per second)
$\hat{p}$	non-dimensional roll rate (pb/V)
q	Safe separation distance power law for following aircraft wingspan
R	Encounter rate
r	Vortex radius
r_C	Vortex core radius
S	Small class
SS	Supersmall class
TATCA	Terminal Air Traffic Control Automation

t_1	Time before vortex decay starts
t_0	Mean time before vortex decay starts
UK	United Kingdom
US	United States
$v(r)$	Vortex tangential velocity profile
V	True Airspeed
VFR	Visual Flight Rules
W	Aircraft mass
$\Gamma(r)$	Vorex circulation profile
Γ_∞	Asymptotic vortex circulation for large radius
Γ'	Average vortex circulation
Γ'_T	Average circulation hazard limit
ϵ	Fraction of vortices not yet starting to decay
ρ	Air density
σ	Standard deviation of time vortex decay starts

1. INTRODUCTION

One of the long term objectives of the Federal Aviation Administration (FAA) Wake Vortex Program has been to mitigate the reduction in runway capacity caused by necessary, but often conservative, wake-vortex separation standards. For example, in FY91, the Program adopted the specific goal of reducing the Heavy-Heavy landing separation from four to three miles. One goal of this report is to examine the options relating to such a reduction. Many other options for reduced separation standards will also be examined.

1.1 BACKGROUND

Any reduction in separation standards must be shown to be safe. The safe separation model[1] that forms the basis for this report is composed of a vortex encounter hazard model combined with a vortex decay model. A static hazard model was used that relates the severity of an encounter to the ratio of (1) the maximum vortex-induced rolling moment to (2) the aircraft roll control capability (see Appendix A). The decay model was derived from vortex measurements using a sodar. The model calculates the probability of a vortex remaining hazardous as a function of the separation time. This probability was found to be greater than zero for existing separation standards that, when observed, had successfully prevented wake vortex accidents. Thus, an acceptable hazard probability was defined by the calculated hazard probability for commonly used aircraft separations, namely the DC-9 and B-737 behind the Large DC-8 at three nautical miles. This model is described in Section 2.2.2 and applied in Chapter 3.

This safety methodology was used to assess whether the Heavy DC-8s and B-707s could be safely classified as Large. The weights of different models of these aircraft span the 300,000-lb boundary between the Large and Heavy classes. The first analysis[2,3] showed that the reclassification was safe for landing. The second analysis[4] showed that the reclassification would also be safe for takeoff.

The original safe separation model was based on vortex decay data for particular aircraft types that were in the fleet when the decay measurements were made (1976-77 for landing, 1980 for takeoff). In the mid 1980s the model was extended to permit the classification of any aircraft type. This work was never published and is now described in Section 2.2.4 and applied in Chapter 5.

The next development[5] in the use of the safe separation model defined levels of safety, rather than using the fixed level of safety associated with DC-9/B-737 operations behind Large DC-8s. Since this pair of aircraft occurred frequently in the traffic mix of the 1970s and early 1980s, its calculated hazard probability was assigned a safety level of "A." The highest calculated hazard probability was for 20-meter wingspan Large aircraft following the DC-8. Since this combination occurred much less frequently in normal operations than the DC-9/B-737|DC-8 combination, its safety is less certain and was therefore assigned a lower safety level of "C." The safety of new separations can be graded by comparing the calculated hazard probability with the A and C levels. Two cases were examined: 2.5-mile separations for Small and most Large aircraft and 3-mile separations between Heavy aircraft (see Sections 3.3 and 3.4, respectively). Note that the

frequency of the C level aircraft combination has perhaps increased in the 1990s with the increase in commuter traffic at many major airports and the B-757 replacing the DC-8 in the traffic mix.

In 1990 lidar and sodar data were first collected[6] for the same wake vortices. The vortex strengths (average circulation) derived from the two types of measurements were found to disagree dramatically because of the much poorer spatial resolution of the sodar. The measurements could be reconciled[7] by using a different strength parameter, which ignores data from the vortex core. This change is compatible with a corresponding improvement in the static hazard, which originally considered a wing centered in the vortex flow field; in fact, real aircraft would also have a fuselage that would be located in the vortex core region. The original separation model[1] included a sensitivity analysis that considered the effect of the poor sodar spatial resolution on the safe separation analysis for small following aircraft. The new, alternative strength parameter changes the safe separation model by assuming the worst case for Small following aircraft and hence replaces the sensitivity analysis of the original model. The alternative safe separation model is described in Section 2.2.4 and applied in Chapter 4.

In 1994, in response to two VFR accidents of business jets following the B-757, the FAA temporarily increased the IFR spacings for all aircraft behind the B-757 by one mile. A Wake Turbulence Aircraft Classification and Separations Standards Industry Team was formed to advise the FAA about how to deal with the two accidents and how aircraft should be classified and separated on final approach. A Science of Separation Distances Subcommittee was tasked to examine the scientific bases for defining aircraft safe separations. The alternative separation model was used for this purpose (Section 4.2). A second separation model[8] was derived from UK encounter statistics (see Appendix B). The Industry Team report was delivered on June 13, 1995, and suggested possible three- and four-class aircraft classification options. The two separation models were used to evaluate the safety of a specific version of the four-class option (see Section 4.6).

In August of 1996, the FAA issued final changes in aircraft separation standards. In addition to the increased separations behind the B-757, the breakpoint between the Small and Large classes was raised to make sure that most business jets are in the Small class. Most of the analyses of this report pertain to the separation standards in use from the mid 1970s until 1994. Since these standards were used for two decades and we have little experience with the new 1996 standards, the 1976-1994 vortex separations represent the bulk of our operational experience with separation standards. Although theoretical analyses are useful, operational experience is the most convincing basis for assuring the safety of possible future reductions in separation standards.

1.2 REPORT OUTLINE

This report reviews available methodologies for scientifically defining safe separation standards and then applies them to a number of specific cases. This chapter provides background information about separation standards. Chapter 2 describes several safe separation models based on empirical vortex decay data for landing aircraft. Chapter 3 uses the original landing safe separation model to analyze the safety of a number of possible classification changes. Chapter 4 uses the alternative landing separation model and the UK encounter model to analyze aircraft

2

Wake Turbulence Aircraft Classifications and Separations Standards Industry Team. Chapter 5 describes a different method of classifying aircraft based on vortex measurements for both landing and departing aircraft. Finally, Chapter 6 discusses the status of the safe separation models.

1.3 SEPARATION SYSTEM REQUIREMENTS

A wake vortex aircraft classification/separation system must meet the requirements discussed in the following sections. The primary focus of these requirements is the separation standards themselves, not the operational procedures making use of the standards. Thus, the issues of efficiency and fairness assume that the aircraft mix and first-come first-served philosophy are constraints. Greater efficiency may result if these constraints are relaxed. Whether such changes are fair or not is outside the scope of this discussion.

1.3.1 Safety

The primary requirement is that the system be safe. This general requirement translates into the specific requirement that no wake-vortex caused accidents will occur when the system is used. For example, since the United States system used prior to 1994 was used for about 18 years with no vortex-caused accident when the vortex separations and procedures were followed, this requirement implies an accident rate of less than one per 18 years. If an accident were to occur, it is likely that the separation standards would be increased. In fact, the standards were increased in 1994 in response to two accidents; however, the accidents did not occur under conditions where the separation standards are applied.

A secondary requirement is that wake vortex encounter incidents be infrequent. Changes in the system should not significantly increase the incident rate.

1.3.2 Efficiency

The system must use available airspace efficiently. The separations used must not be overly conservative. The separations should reflect the actual duration of the wake vortex hazard for each generator/encounterer pair as closely as possible, so that unnecessarily large separations are avoided. The efficiency of the system is optimized when:

a)   Enough wake vortex classes are used to accurately fit the actual hazard duration.

b)   Separations are reduced until the maximum acceptable incident rate is reached.

This prescription is valid under the constraints of first-come first-served runway use and no change in aircraft mix.

1.3.3 Fairness

A fair system will result in a wake vortex incident probability per operation that is comparable for all classes of following aircraft. A system may not be acceptable just because the overall incident rate is reasonable; for example, most of the incidents could occur for one class of aircraft. It should be noted that a fair system is also likely to be efficient, within the constraints of this

3

discussion, since the prescription for efficiency in Section 3.2 would lead to the same incident rate for all aircraft.

1.3.4 Complexity

The system must not be too complex to be used operationally. The number of classes and separations must be small enough for easy use by air traffic controllers. Changes in the separation standards cannot significantly increase controller workload unless some means is provided to help carry the load. An automated spacing system might be able to provide the assistance needed to handle a more complex standard with many classes and finer resolution separations, i.e., fractions of nautical miles rather than integer values. The installation of such a system poses additional requirements concerning its costs and benefits. The gain in capacity must be worth the cost. Wake vortex capacity increases would be only a part of the total benefit of such a system.

1.3.5 Class Boundaries

The boundary limits between wake vortex classes are, to a considerable extent, arbitrary. The safe wake vortex separation for a particular generator/follower pair depends upon three sets of parameters:

a)   Parameters of the generating aircraft, such as wingspan, engine placement, weight, airspeed, flap setting, engine thrust, etc.;

b)   Parameters of the following aircraft, such as wingspan, roll-control authority, airspeed, altitude, etc.; and

c)   Parameters of the atmosphere, such as wind speed, wind direction, wind shear, thermal stability, turbulence level, etc.

Because of variations in aircraft parameters such as weight and airspeed, not to mention variations in meteorological parameters, the safe separation is not a well defined function of a single parameter such as maximum certificated gross takeoff weight, but is better described as a "broad-brush" relationship with considerable spread. In general, the safe separation distance increases with increasing size of the generator and decreases with increasing size of the follower.

Increased wake vortex separations are needed whenever the safe wake vortex separation is larger than the separation mandated for other safety considerations, which is currently 3 nm. In principle, this requirement can be met by a variety of different breakpoints for generator and follower classes. In practice, the wake vortex breakpoints have been set on the basis of other criteria for classifying aircraft. For example, the Heavy class was first defined when the new wide-body aircraft were introduced into service. The 300,000 lbs breakpoint was designed to place all newly introduced heavier aircraft into the Heavy class. This selection of the breakpoint placed some models of DC-8 and B-707 aircraft in the Heavy class while others remained in the Large class. The original Small class breakpoint (12,500 lbs) stems from the era when there was a large weight difference between the transport category aircraft such as the DC-3, Convair 440, etc., and the majority of general aviation aircraft which were much lighter than 12,500 lbs. What is now the Large wake vortex class was originally the transport aircraft category. The historical

4

criteria for setting wake vortex class boundaries were not primarily concerned with wake vortex characteristics; available wake-vortex data were used only to define the required separations. Consequently, it is likely that a better set of classes can be defined if wake-vortex criteria are applied to both class and separation definitions.

The optimum (i.e., most efficient use of airspace) classification scheme depends upon the mix of aircraft as well as the wake vortex characteristics of generating and following aircraft. The classes should be defined so that the most common aircraft have the smallest separations. For example, if a hub airport primarily serves jet transport aircraft of the DC-9/B-737 size and larger, it makes no sense to use a spacing for a DC-9 behind a B-747 that would be safe for a much smaller following aircraft.

Once a particular classification scheme has been introduced, wake vortex safety becomes defined in terms of the historical experience with the particular scheme and it becomes difficult to make changes without convincing evidence, *especially for reduced separations*. A thorough safety analysis and a carefully monitored implementation period would be required to assure that the new separations are safe.

1.4 UNITED STATES SEPARATION STANDARDS

The operational U.S. wake-vortex separation system consists of two parts:

    1)   Aircraft classes, and

    2)   Minimum aircraft separations for aircraft pairs based on their assigned classes.

1.4.1 Aircraft Classes

Table 1 shows the first aircraft wake-vortex classification system adopted by the United States around 1970. Aircraft are assigned to one of three classes, Small, Large or Heavy, based on the maximum certificated gross takeoff weight (MCGTOW). This system was used without exception until July 1994. The selection of 300,000 lbs as the breakpoint between the Large and Heavy classes resulted in different models of the B-707 and DC-8 (with MCGTOW on either side of the breakpoint) being in different classes. Although studies[2,3,4] showed that the Heavy versions of these aircraft could be safely classified as Large, no decision was made as most of the affected aircraft were retired from service in the U.S. and the question was no longer relevant.

Table 1. Original Wake Vortex Aircraft Classes: Limits on MCGTOW

Wake Vortex Class	Lower Weight Limit (lbs)	Upper Weight Limit (lbs)
Small	0	12,499
Large	12,500	300,000
Heavy	301,000	none

The B-707 and DC-8 were replaced by the B-757, which is definitely below the 300,000 lb breakpoint, and the B-767, A-300 and A-310, which are definitely above the breakpoint. In 1994, as a consequence of two VFR accidents involving following business jets, the United States

adopted an interim reclassification of the B-757; the separation for all following aircraft was increased by one nautical mile.

In 1995, the FAA requested that the aviation industry convene a team to review the aircraft classification and recommend changes in the classification system. Based on the task force report and other considerations, the classification system shown in Table 2 was adopted in August 1996. The primary goal of the changes was to reduce the size range of aircraft assigned to the Large class (from a factor of 24 to a factor of 6.2 in MCGTOW). Although not formally defined as a separate class, the B-757 was effectively placed in its own wake-vortex class.

Table 3 shows how the change in aircraft classification affected different weight groups based on MCGTOW. The former Large class is actually split into all four of the new classes.

Table 2. Current Wake Vortex Aircraft Classes: Limits on MCGTOW

Wake Vortex Class	Lower Weight Limit (lbs)	Upper Weight Limit (lbs)
Small	0	41,000
Large	41,001	255,000
B-757		
Heavy	255,001	none

Table 3. Changes in Vortex Aircraft Classes for MCGTOW Groups

Weight Group	Lower Weight Limit (lbs)	Upper Weight Limit (lbs)	Current Class	Former Class
S1	0	12,500	Small	Small
S2	12,501	41,000	Small	Large
L	41,001	255,000	Large	Large
B-757	220,000	250,000	B-757	Large
H1	255,001	300,000	Heavy	Large
H2	300,001	none	Heavy	Heavy

1.4.2 Minimum Aircraft Separations

Table 4 shows the U.S. final approach IFR landing radar minimum separation standards that were finalized in the mid 1970s and used until July 1994. The first entry of each block in the table is the minimum required separation distance (nautical miles, nm) at runway threshold for the leader-follower class pair. The corresponding separation times are also listed, assuming a nominal landing airspeed of 135 knots.

Table 4. IFR Separation Standards at Runway Threshold before 1994

Leading Aircraft Class	Following Aircraft Class		
	Heavy	Large	Small
Heavy	4 nm, 107 sec	5 nm, 133 sec	6 nm, 160 sec
Large	3 nm, 80 sec	3 nm, 80 sec	4 nm, 107 sec
Small	3 nm, 80 sec	3 nm, 80 sec	3 nm, 80 sec

The basic radar separation is 3 nm; the larger separations in Table 4 are based on wake vortex considerations. The 3-nm radar separation was originally based on the resolution of the radar display, which has been subsequently improved. However, it also protects against other problems, including wake-vortex encounters. Any reduction in the basic radar separation must be safe from all points of view. For example, starting in the 1980s, airports with short runway occupancy times were permitted to use 2.5-nm separations for certain equal sized aircraft. Although runway occupancy was the primary criterion in this reduction, wake vortex safety also had to be considered (see Sections 1.6.3 and 3.3).

The separation standards in Table 4 provided vortex-accident-free IFR operations for almost two decades when the procedures are followed:

1)   Spacings no smaller than minimums, and

2)   Leading and following aircraft remain on the glideslope, as recommended by the Airmen's Information Manual.

These separations can, therefore, be considered safe for the common aircraft in the fleet. It should be noted, however, that the fraction of aircraft at the lower end of the Large class in Table 1, specifically commuter aircraft, has increased greatly in recent years. The safe separation model presented in Section 3.1 suggests that these aircraft may have the highest risk of a wake vortex encounter with the separation standards of Tables 1 and 3.

The 1996 change in classification adopted the IFR landing minimum separations shown in Table 5. For simplicity, only the distance separations are listed. Any spacing of 3 nm can be reduced to 2.5 nm for short runway occupancy times. The net effect of these changes is to increase the spacing of business jets behind the B-757 from three to five nautical miles.

Table 5. 1996 Wake Vortex IFR Separation Standards at Runway Threshold

Leading Aircraft Class	Following Aircraft Class			
	Heavy	B-757	Large	Small
Heavy	4	5	5	6
B-757	4	4	4	5
Large	3	3	3	4
Small	3	3	3	3

Table 6 lists the separation changes for the weight groups listed in Table 3. The separations are increased for all aircraft behind the B-757 and the H1 group. Only two decreases in separation are noted, S1 behind S2 and H1 behind H2. Note that there are no aircraft in the current fleet in group H1.

Table 6. Separation Changes for Weight Groups

Leader Weight Group	Follower Weight Group					
	H2	H1	B-757	L	S2	S1
H2	0	-1	0	0	+1	0
H1	+1	+1	+2	+1	+3	+2
B-757	+1	+1	+1	+1	+2	+1
L	0	0	0	0	+1	0
S2	0	0	0	0	0	-1
S1	0	0	0	0	0	0

1.5 SEPARATION PHILOSOPHY

The recent discussions and changes in separation standards highlighted a number of philosophical issues concerning classification and separation standards.

1.5.1 Vertical Versus Longitudinal Separations

The traditional interpretation of the longitudinal IFR landing separation standards assumed that aircraft are following normal IFR procedures of flying on the glideslope. It has been known since the original Heavy aircraft wake vortex flight tests in 1969 that, away from the ground, wake vortices can last much longer than the time spacings provided by radar separation standards. The separations are safe, however, for aircraft flying on the glideslope because wake vortices normally descend below the flight path of the generating aircraft. Vortices generated near the ground cannot reliably descend below the glideslope and hence are the limiting factor in defining longitudinal separation standards. Fortunately, vortices generally decay faster near the ground. This picture of the vortex encounter hazard is the basis for the vortex decay models presented in Section 2.2, which are based on vortex decay measurements between the middle marker and the runway threshold.

In VFR operations, aircraft are not constrained to remain on the glideslope and it is possible for wake vortex encounters to occur at the normal IFR separations. The two business jet accidents behind B-757s occurred when their flight paths were below the flight path of the B-757. Most of the recommendations of 1995 industry team were intended to keep VFR aircraft on the same glideslope used for IFR operations. The FAA, however, decided to prevent VFR accidents by increasing IFR longitudinal separations rather than controlling VFR vertical separations. This approach is costly in terms of airport capacity for two reasons:

1) The required increase in longitudinal separation is quite large.

2) IFR capacity is sacrificed for VFR safety. Major airports typically have excess VFR capacity, but are short on IFR capacity.

1.5.2 Weight Versus Wingspan

The 1996 classification changes continued to use the traditional MCGTOW classification parameter. However, as discussed Section 2.1, wingspan is the best single-parameter indicator of how an aircraft responds in a wake vortex encounter. The use of a better indicator of wake vortex hazard should give greater efficiency for the separation system. This efficiency improvement can be demonstrated for the Small-Large boundary:

Figure 1 plots the weight versus the wingspan for aircraft listed in the 1993 Official Airline Guide (OAG). For the same weight, propeller aircraft generally have longer wings and, hence, less encounter upset risk than jet aircraft. Two possible boundaries between the Small and Large class are plotted:

- Wingspan = 60 feet

- Weight = 41,000 lbs
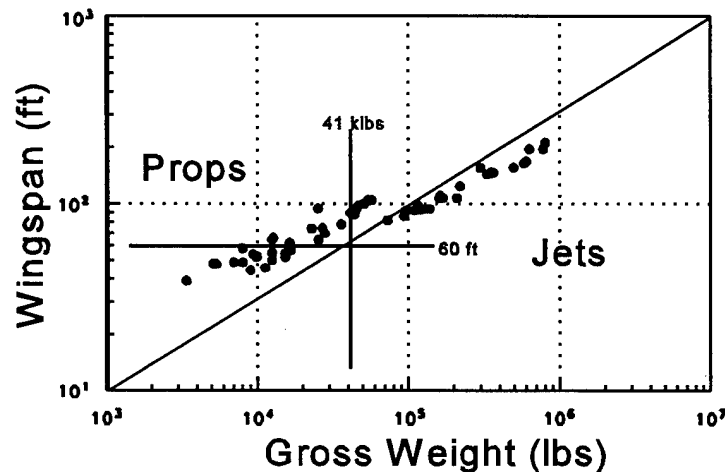
Figure 1. OAG Aircraft Types: Wingspan vs. Weight

The wingspan boundary places a number of commuter propeller aircraft in the Large class that would be placed in the Small class using the weight boundary. The wingspan classification would require less spacing for these commuter aircraft behind the Large jet transport aircraft that form the bulk of the traffic at most major airports and hence would result in greater airport capacity.

1.6 SEPARATION METHODOLOGIES

Three methodologies have been used in the United States to define safe separation standards. Over the years some separations have been increased. However, separations have rarely been decreased; the two instances are:

    1)   The 2.5-mile spacing for similar sized aircraft and short runway occupancy times (see Section 1.6.3), and

    2)   The August 1996 changes (Table 6) where the reduction was the result of increasing most separations while retaining only three generic aircraft classes.

In both of these instances, the changes were made for a limited range of aircraft sizes where wake vortex considerations are expected to be unimportant. The challenge is to develop separation methodologies to the level of acceptance that separations can be routinely decreased when appropriate for separations known to depend upon wake vortex considerations.

1.6.1 "Worst Case" Methodology

The original U.S. wake vortex instrument flight rules (IFR) separation standards (1969) were based on vortex encounter flight tests carried out under "worst case" conditions (low turbulence at high altitude). Because the resulting worst case separation standards would have severely reduced airport capacity, the separations adopted were reduced from those indicated by the flight tests. Part of the justification for this reduction was that higher turbulence levels are expected near the ground. [In 1975, separations for Small aircraft were increased by one mile as a result of wake-vortex measurements near the ground. Table 4 reflects this increase.]

Operational experience for the 18 years prior to 1994 indicate that the separations standards presented in Tables 1 and 4 are safe; no accidents have occurred when the required IFR separations and procedures (e.g., fly at or above the glideslope) have been observed.

Since the most critical region for wake vortex encounters is near the ground, the apparent contradiction between "worst case" flight tests and operational experience has generally been explained as the consequence of faster vortex decay near the ground. This hypothesis is more difficult to support, however, in light of measurements taken at airports in 1976-1980[1,4] and in recent[6] vortex measurements. According to the hazard model (see Appendix A) used for analyzing such data, the vortex appears to persist longer than the current separation standards under "worst case," low turbulence conditions, just as observed in tests at altitude. If the hazard model can be validated, this observation leads to three conclusions: 1) worst case conditions cannot be used to set realistic separation standards; 2) worst case conditions must be rare in operational scenarios; and 3) safety would be enhanced if the rare worst case meteorological conditions could be identified and increased separations employed under these conditions.

1.6.2 "Normalized Safety" Methodology

An alternative procedure[9] for setting separations from wake vortex measurements is based on the assumption that the current separation standards are "safe." A vortex hazard model is used to assess the hazard threshold for vortex strength. Vortex decay measurements are processed to give an empirical model for vortex decay, which specifies the probability of the vortex strength remaining above a given value as a function of vortex age. These two models can be combined to determine the vortex hazard probability at a given separation time. If the hazard probability under current standards for a frequently occurring aircraft pair is defined as safe, then the safe separation times for other aircraft pairs can be determined. The sensitivity of the results to the assumed hazard model must then be assessed. This methodology is the basis of this report; its development and application was outlined in Section 1.1.

Note that this methodology is contrary to the often stated philosophy for wake vortex avoidance that "the only acceptable level of wake vortex encounters is *zero*." Such a goal is unrealistic and, if pursued seriously, would dramatically reduce airport capacity (see Section 1.6.4).

1.6.3 "VFR Comparison" Methodology

In most operational situations, the separations selected by pilots under Visual Flight Rules (VFR) operations are less than those required for IFR operations. This difference has been used to

indicate how separations might be reduced and was one of the factors* used to justify the 2.5-mile IFR separation for like aircraft smaller than the Boeing 757. After all, the response of the aircraft to a wake-vortex encounter is the same in IFR as in VFR. There are some differences between VFR and IFR, however, that might affect safe separations:

1) The air traffic controller, rather than the pilot, is responsible for maintaining separations under IFR. Controllers may maintain an extra spacing buffer to prevent separations from decreasing below the spacing minima.

2) Under VFR the pilot can see the preceding aircraft and can take wake-vortex avoidance precautions (such as staying above the glideslope and/or landing long).

3) The pilot may be able to respond more quickly to a wake vortex encounter in VFR since he/she is relying on visual rather than instrument indications of roll attitude.

1.6.4 Encounter Reporting System

The United Kingdom has adopted a somewhat different approach to the wake vortex problem than the United States. A wake-vortex encounter reporting system[10,11] has been in operation since 1972. The information from this system has been used to make numerous changes in aircraft separations, both increasing and *decreasing*. One method of validating a wake-vortex separation model would be to accurately predict the observed UK incident rates, assuming that they are actually caused by wake vortices and not other phenomena such as wind shear. A mathematical model was developed[8] to fit the UK 1982-1990 encounter data; Appendix B outlines this model. This model predicts that landing encounters of DC-9/B-737 aircraft behind the B-757 would disappear if the separation were increased from three to five miles.

Note that the UK operational experience will not be used to normalize the safe separation models developed in this report. The UK experience cannot compete with the U.S. 18-year experience with consistent standards for two reasons:

1) The separations have changed too often.

2) The number of capacity limited airports is much smaller.

---

*A short test (500 operations) was also conducted at several airports to assess whether the shorter separations caused wake vortex encounters.

2. WAKE-VORTEX SEPARATION/CLASSIFICATION MODELS

The wake-vortex separation model consists of a vortex hazard model and a vortex decay model.

2.1 VORTEX HAZARD MODEL

The development history and validation efforts for the vortex hazard model are presented in Appendix A. Enough information is presented in this section to permit an understanding of the various separation models.

2.1.1 Summary

The hazard model estimates the hazard caused by vortex-induced roll on a following aircraft. The basic parameter of the model is f, the ratio of the largest acceptable induced rolling moment to the roll control authority of the encountering aircraft. For example, if f is set at 0.90, the pilot can safely control the aircraft until the induced roll exceeds 90 percent of the roll control authority. If one considers pilot reaction times and other factors, the effective value for f may be as low as 0.5[12]. The value of f can be varied to determine the sensitivity of the analysis to the choice of this basic parameter. The result of the hazard analysis is that a vortex is hazardous if its average circulation (evaluated for a radius equal to half the wingspan of the following aircraft) is above a threshold value which is proportional to f.

2.1.2 Details

The goal of the hazard model is to relate the maximum safe vortex-induced rolling moment on the wing of the encountering aircraft to the strength of a wake vortex from a leading, vortex-generating aircraft. Studies have shown that the largest torque occurs when the wing is centered in the wake vortex. Under the additional assumptions of the model, the torque on a wing of span b is proportional to the integral of the vortex circulation profile $\Gamma(r)$ over the wing:

$$\Gamma'(b/2) = (1/b) \int_{-b/2}^{b/2} \Gamma(r) \, dr \qquad (1)$$

where r is the vortex radius, b is the wingspan of the encountering aircraft, and $\Gamma'(b/2)$ is the average vortex circulation. For an axially symmetric vortex, the circulation profile $\Gamma(r)$ is related to the vortex tangential velocity profile $v(r)$ by:

$$\Gamma(r) \equiv \oint \mathbf{v \cdot dl} = 2\pi \, r \, v(r), \qquad (2)$$

where $\mathbf{v}$ is the velocity vector and $\mathbf{dl}$ is the distance increment vector. Since the term "vortex strength" is sometimes applied to the circulation $\Gamma(r)$, in particular the limiting value Γ_∞ as r approaches infinity, $\Gamma'(b/2)$ in Equation 1 will often be referred to as the "average strength."

The notable feature of Equation 1 is that the torque depends only upon the average circulation, but not on the shape of the velocity profile producing the average circulation. This independence

13

of the velocity profile can be used in a mathematical trick (see Section A.1 in Appendix A) to relate the average vortex strength hazard threshold Γ'_T to the maximum nondimensional roll control $\hat{p}$ of the encountering aircraft and the fraction f of the roll control that can be used to counter a wake-vortex upset:

$$\Gamma'_T(b/2) = (\pi/3)fbV\hat{p}, \tag{3}$$

where V is the airspeed and $\hat{p}$ is nondimensional roll rate, which is typically 0.06 for commercial aircraft and 0.08 for general aviation aircraft. A value of f in the range of 0.5 to 1.0 is typically used to represent the wake vortex hazard. Much of the data analysis using this hazard model has used the expression:

$$\Gamma'_T(b/2) \approx 5fb \quad (m^2/s), \tag{4}$$

which is consistent with the nominal values for landing jet transport aircraft (V = 130 knots (68 m/s) and $\hat{p}$ = 0.07). The exact expression of Equation 3 must be used when the product $V\hat{p}$ is significantly different from these values.

The left side of Equation 3 can be evaluated using what has been termed[1] the "simple" vortex model, which gives the appropriate tangential velocity variations at both small (~r) and large (~1/r) radii:

$$\Gamma(r) = \Gamma_\infty/[1 + (r_c/r)^2], \tag{5}$$

where r_c is the vortex core radius and Γ_∞ is the asymptotic vortex circulation for large radius r. Using the vortex circulation profile in Equation 5, the integral of Equation 1 can be carried out analytically to yield:

$$\Gamma'(r) = \Gamma_\infty[1 - (r_c/r)\tan^{-1}(r/r_c)]. \tag{6}$$

2.2 VORTEX DECAY MODELS

Reference 1 developed three wake-vortex decay models based on measurements taken on landing aircraft at Chicago O'Hare airport in the late 1970s using the Monostatic Acoustic Vortex Sensing System (MAVSS). Appendix C outlines these three models and also presents corrections to Reference 1. In accordance with the vortex hazard picture presented in Section 1.5.1, the MAVSS landing data were collected for two runways, 32L and 14R, at distances of 655 and 503 meters, respectively, from the runway threshold.

In 1980 MAVSS measurements were collected on aircraft taking off from Chicago O'Hare airport[4]. Section 2.2.4.2 will present an analysis of vortex decay using one of the three models for both landing and takeoff measurements.

The data for both landing and takeoff were collected during normal working hours and therefore represent daytime vortex decay, which is often dominated by turbulence. At the time of data collection the strong effects of meteorology[13] on vortex decay were not fully appreciated.

2.2.1 MAVSS Data Characteristics

The MAVSS[14] measures the velocity profile of a vortex as it passes over a fixed, vertically pointing acoustic radar. A series of antennas is installed on a baseline perpendicular to the flight path. Vortex measurements at successively greater vortex ages are obtained as the vortex passes over each antenna in the series. Because of limited spatial resolution and other problems[2,7], the MAVSS cannot resolve the core velocities of most wake vortices.

The MAVSS data are processed to yield the average vortex circulation out to radii of 5, 10 and 20 meters for each vortex detection. If a vortex is not detected at an antenna at approximately the time expected from the arrival times at antennas closer to the runway centerline, then the vortex strength is assumed to be zero at that expected arrival time unless the vortex detection would be obscured by the arrival of the next aircraft. The MAVSS data thus yield a history of vortex average circulation for the two vortices: Vortex 1 which is the first to arrive at an antenna (the downwind vortex) and Vortex 2 which is the second to arrive (the upwind vortex).

The vortex hazard model defines a hazard threshold for the average circulation for a radius equal to half the wingspan of the encountering aircraft. The MAVSS average circulation histories are processed at 10-second intervals to determine what fraction of the vortices remain above the hazard threshold as a function of vortex age. This fraction is defined as the "hazard probability." For old vortices this probability decays as the square of the vortex age. A variety of mathematical models were investigated[1] to fit the probability decay curves (see Appendix C).

2.2.2 Separation Model

The separation model makes use of the simple stochastic decay model of Reference 1 (see Appendix C). Vortex 2 is observed to last longer than Vortex 1 and is also the vortex that will linger near the runway centerline to pose a possible hazard to the next aircraft. Therefore, data on Vortex 2 is used in the separation model to analyze the safety of longitudinal vortex separation standards.

The simple stochastic model uses two parameters to represent the decay of hazard probability with vortex age. The first parameter is the initial vortex strength, which is taken as the mean average circulation at vortex age 10 to 15 seconds. The second parameter is a decay time parameter. The two parameters were fitted to the decay measurements for each aircraft type and three circulation averaging radii: 5, 10, and 20 meters. The computer code for the separation model is presented in Appendix D. The code contains the model parameters, which were taken from Reference 4 and will not be repeated here.

The methodology of Reference 1 was modified somewhat to produce the tables in Section 3:

1)   Previously the average circulation for 15-meter averaging radius was obtained by averaging the values for 10- and 20-meter averaging radii. Here the average circulation values for 15, 25 and 30 meters are obtained by fitting the 10 and 20

15

meter values to the analytical vortex model of Equation 6. The 20-meter decay time parameter was used for 25 and 30 meters.

2) Some round-off errors were eliminated.

The use of the separation model for small following aircraft (e.g., 10 meter wingspan) is subject to possible errors because of the poor spatial resolution of the MAVSS (discussed in Section 2.2.1). Reference 1 showed how to take these possible errors into account. The analyses presented in Chapter 3 will not consider such errors and hence may not be valid for small following aircraft. The alternative separation model presented in the next section is the most satisfactory way of dealing with the MAVSS measurement limitations.

2.2.3 Alternative Separation Model

2.2.3.1 Rationale

The traditional calculation (Equation 1) of the vortex-induced rolling moment on the wing of an encountering aircraft assumes that the wing extends from the aircraft axis to the wingtip. The result of the calculation (Equation 3) is that the rolling moment is approximately proportional to the average vortex circulation integrated from the vortex axis out to radius $b/2$.

This picture of the vortex encounter has two problems:

1) The effect of the fuselage of the encountering aircraft is ignored.

2) The measurement results for small encountering aircraft are strongly dependent upon instrumental errors in measuring the vortex core. In fact, no existing instrumentation effectively resolves the vortex core for all aircraft. Moreover, some of the most useful vortex decay data, namely the MAVSS data, has relatively poor spatial resolution.

These problems can be resolved by characterizing the vortex by its total circulation Γ_∞ rather than its average circulation, as is done in Greene's out-of-ground-effect vortex decay model[13]. The following rationale is offered for making this change:

1) Lidar studies[15] of vortex decay have shown no evidence for vortex decay significantly increasing the core size. Moreover, the main effect of vortex decay is to make the circulation constant outside the vortex core.

2) For most pairs of aircraft the vortex core is smaller than the size of the fuselage. The core size therefore has less impact than the fuselage size. The vortex center problem therefore belongs to the encounter model rather than the decay model.

The practical effect of changing the split between vortex characterization and encounter modeling is to simplify the characterization of vortex strength to a single parameter Γ_∞. Existing data on average circulation can be processed to give a best estimate for Γ_∞. This processing has been shown[7] to eliminate the large average circulation differences noted between laser doppler velocimeter (LDV) and MAVSS results.

16

2.2.3.2 Circulation

The alternative hazard model will use Γ_∞ in place of Γ^n in Equations 3 and 4. Equation 4 becomes particularly simple; the hazard threshold for Γ_∞ is proportional to the wingspan of the following aircraft. No other dependence on the wingspan of the following aircraft is required.

The alternative decay model will use the initial vortex circulation calculated using the 10- and 20-meter average circulations (listed as measured values in Table 7) and the decay time constant for 10-meter averaging radius. The decay rate for a small averaging radius was selected because the decay is typically faster for larger averaging radii. This choice gives a suitable estimate of vortex decay for small following aircraft.

2.2.4 Classification Model

Since the purpose of the classification model is to classify all aircraft, even those for which no wake vortex data exist, the classification vortex decay model attempts to fit the observed vortex decay to a small number of aircraft parameters. The model can then be applied to any aircraft type. The aircraft classification model to be presented accepts parameters describing a particular aircraft and outputs a classification such as Small, Large, or Heavy.

The current classification model uses a single parameter, maximum certificated gross takeoff weight (MCGTOW) to classify an aircraft for wake-vortex related separation standards. Empirical evidence[1] indicates that engine placement should also play a role in aircraft classification. The wake-vortex hazard appears to persist somewhat longer behind landing aircraft with two wing-mounted engines than would be expected based on aircraft size alone. This section, therefore, will develop a vortex decay model based upon both aircraft size (wingspan) and engine placement. The model will consider both landing and takeoff operations even though most reported vortex incidents are during aircraft landings. The model will use both analytic methods and fits to empirical data collected at Chicago O'Hare airport.

In order to deal with all possible generating aircraft, the classification model uses total circulation as the strength parameter. However, in contrast to the alternative separation model of Section 2.2.3, it calculates the encounter severity using average circulation based on an assumed core radius (see Equation 16 in Section 5.1). In the absence of vortex measurements, such assumptions are necessary to predict the vortex hazard for any aircraft type.

2.2.4.1 Initial Vortex Strength

According to aerodynamic theory the total initial vortex circulation is given by:

$$\Gamma_\infty(0) = (KWg)/(\rho BV), \tag{7}$$

where

$\quad \Gamma_\infty(0) \quad$ = vortex strength at time zero (m^2/s)
$\quad K \qquad$ = nondimensional wing-loading constant equal to unity for uniform loading and

4/π for elliptic loading

W = Aircraft maximum landing mass (Kg)

g = Gravitational acceleration (9.82 m/s²)

ρ = Air density at sea level (1.28 Kg/m³)

B = Aircraft wingspan (meters)

[Note that B will be used as the wingspan of the generating aircraft and b as the wingspan of the following aircraft.]

V = Landing speed (m/s)

Table 7 shows generally good agreement between the strengths predicted by Equation 7, assuming uniform wing loading (K = 1.00), and the initial vortex strengths measured by the MAVSS system during the Chicago O'Hare landing data collection (Reference 2). For any given aircraft type, an average over all models of that type was used for W, B, and V in Equation 7. Note that, in Table 7, the measured strengths for most aircraft with four wing-mounted engines would show better agreement with the larger predicted strengths given by a value of K midway between 1.00 and 4/π.

Table 7. Initial Landing Vortex Strength (m²/s)

Aircraft Type	Analytic Γ_∞	Measured Γ_∞
B-737	212	203
DC-9	203	200
B-727	246	249
B-707	225	259
DC-8	236	298
B-707H	245	249
DC-8H	264	289
L-1011	366	354
DC-10	394	348
B-747	430	497

Table 8 compares the initial vortex strength measurements for landings and takeoffs at Chicago O'Hare airport. The vortex strengths in Table 8 are median values for the vortex circulation Γ averaged over a 20-meter averaging radius. For each aircraft type, the vortex strength during takeoff is less than the vortex strength during landing. This result is inconsistent with Equation 7 if the wing loading factor K is assumed constant because the ratio W/V is generally greater on takeoff than on landing. This discrepancy may result from the change in lift distribution caused by the greater flap deployment on landing.

Table 8. Comparison of MAVSS Initial Vortex Strengths for Landing and Takeoff

Aircraft Type	Landing (m²/sec)	Takeoff (m²/sec)	Difference (percent)
B-737	136	135	-1
DC-9	130	120	-8
B-727	162	138	-15
B-707	184	166	-10
DC-8H	201	191	-5
L-1011	228	216	-5
DC-10	216	209	-3
B-747	291	260	-10

The data in Table 8 suggest that there may be an engine-placement effect on initial vortex strength. The three aircraft (B-737, L-1011, and DC-10) with two wing-mounted engines show a smaller difference between landing and takeoff vortex strengths than the other aircraft. In the initial strength model for aircraft taking off, the value given by Equation 7 was used for aircraft with two wing-mounted engines. For the remaining aircraft, 0.90 times this value was used.

18

2.2.4.2 Decay

The classification model uses the stochastic vortex decay model outlined in Appendix C. The analysis of Reference 1 for the stochastic model is slightly modified by adopting a decay exponent of $n = 1.5$ rather than $n = 2.0$ used there. Note also that, the model is fitted to the decay of all vortices, not just Vortex 2, as was done in Section 2.2.2. Since this report is the first description of the classification model, more details of the analysis will be presented.

The strengths of vortices have often been observed to remain constant for some time t_1 and then decay rapidly. Accordingly, the model adopted for vortex strength versus time is:

$$\Gamma_\infty(t) = \Gamma_\infty(0) \quad \text{if } t \le t_1 \tag{8}$$

$$\Gamma_\infty(t) = \Gamma_\infty(0)(t_1/t)^n \quad \text{if } t > t_1 \tag{9}$$

where the onset of decay is a stochastic variable normally distributed with mean t_0 and standard deviation σ. The assumption of constant strength followed by a power-law decay may be suitable for decay that is dominated by turbulence, but is not appropriate for the conditions of greatest vortex lifetime[15] where the total circulation is observed to decay but the core remains unchanged.

For each aircraft type, the decay rate parameter n was set to a fixed value and the other two model parameters t_0 and σ were adjusted to best fit the observed vortex average strength distributions at ten-second intervals. The best fit to the observed strength distributions generally occurred for $n=1.5$. The best-fit values for σ were generally close to 10 seconds. The mean value t_0 for the onset of decay varied with aircraft size, being larger for the larger aircraft types. For each aircraft, for both landing and takeoff, four model fits were performed corresponding to

Table 9. Stochastic Decay Model Parameters for 20-m Averaging Radius

Aircraft Type	Landing		Takeoff		t_1 for $\epsilon=0.001$	
	σ	t_0	σ	t_0	Landing	Takeoff
DC-9	11.2	27.8	10.8	23.9	62.4	57.1
B-737	12.1	32.7	6.3	24.6	70.2	44.1
B-727	9.0	28.6	6.0	28.5	56.4	47.2
B-707	10.3	32.0	7.8	33.8	63.9	57.8
B-707H			12.0	33.4		70.4
DC-8	10.0	33.2			64	
DC-8H	10.3	30.2	10.1	30.5	61.9	61.9
L-1011	11.1	39.8	11.0	30.9	74.2	64.8
DC-10	12.7	34.9	10.3	31.6	74.3	63.3
B-747	11.1	40.0	14.4	40.2	74.4	84.7

averaging radii of 5, 10, 15, and 20 meters. All vortices were included in the fit. The best-fit t_o and σ values for the largest averaging radius (20 meters), shown in Table 9, were used in the classification model to characterize the decay of Γ_∞. The vortex velocity profile was assumed to keep the same shape during decay (constant r_c in Equation 5). Since the fit parameters were found to vary little with averaging radius, this approximation should adequately represent vortex decay. The decay fits for the B-707H on landing and the DC-8 on takeoff will not be used since too few cases were observed to give meaningful results. Note that the decay is generally slower on landing.

Results derived from the decay model fits are shown in Figures 2 and 3 for landing aircraft and departing aircraft, respectively. On the vertical axis, the figures show the "decay time" which is defined as the time t_1 at which all but a fraction ϵ of the vortices have begun to decay. Three values of ϵ are included: 0.001 (X, top), 0.01 (+, middle) and 0.10 ($\square$, bottom). [The numbers for $\epsilon = 0.001$ are also listed in Table 9.] The "decay time" defined above is equivalent to the vortex hazard time for a particular hazard probability ϵ if the hazard strength threshold is equal to the initial strength. If a more realistic hazard strength threshold were used, such as half the initial strength, then the "hazard time" would equal a multiple (>1.0) of the "decay time" (see Equation 9). Note that the vortex decay time is characteristic of the vortex generating aircraft and not the hazard to a particular following aircraft.

In Figures 2 and 3 the horizontal axis is the aircraft wingspan. For a given probability level ϵ, the decay time increases approximately linearly with wingspan on the plots. A linear fit was made to the data and the
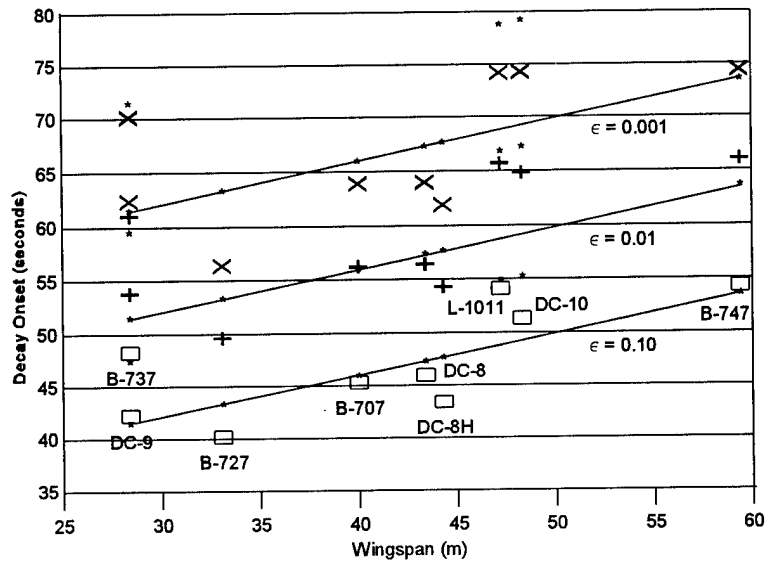
Figure 2. Decay Onset for Landing Data
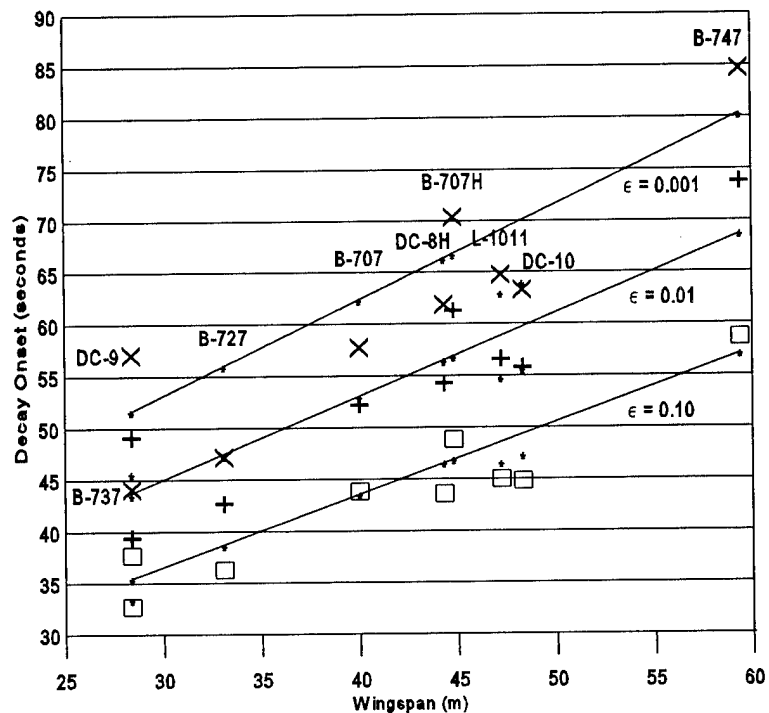
Figure 3. Decay Onset for Takeoff Data

20

fitted lines are drawn on each figure for the three values of ϵ. This analysis shows a greater dependence of decay onset on aircraft size for takeoffs than for landings. Perhaps on landings the proximity of the ground to the vortices plays a more significant role in vortex decay and reduces somewhat the effect of aircraft size.

The equation for the linear fit to the landing data is:

$$t_1(\epsilon,B) = 0.39 B + 10 \log_{10}(1/\epsilon) + 20 \qquad (10)$$

and for takeoff, the equation of the linear fit is:

$$t_1(\epsilon,B) = [0.70+0.11(\log_{10}(1/\epsilon)-1)] B + 5 \log_{10}(1/\epsilon) + 10 \qquad (11)$$

The interpretation of $t_1(\epsilon,B)$ is that for a vortex generated by an aircraft with wingspan B meters, there is a probability ϵ that the onset of vortex decay will be at least t_1 seconds.

The straight lines produced by Equations 10 and 11 are shown in Figures 2 and 3, respectively. The deviations of the individual data points from the fitted lines indicate that engine placement may affect the time delay before vortex decay begins. This effect is most noticeable in the landing plots (Figure 2). In all three of these plots ($\epsilon = 0.10, 0.01, 0.001$), the aircraft with two wing-mounted engines are generally well above the fitted line, indicating that for this engine placement the onset of vortex decay, and hence hazard duration, is 5 to 10 seconds longer than would be expected for an aircraft of the given wingspan. Consequently, an engine-placement term e is added to $t_1(\epsilon,B)$ for any aircraft with two wing-mounted engines. Thus, the expression obtained for the onset of vortex decay is now a function of three variables: ϵ probability level, wingspan B, and engine configuration E. For landing aircraft this expression is now:

$$t_1(\epsilon,B,E) = 0.39 B + 10 \log_{10}(1/\epsilon) + 20 + eE, \qquad (12)$$

where

$$e = 2 \log_{10}(1/\epsilon) + 4 \qquad (13)$$

and E is one for aircraft with two wing-mounted engines and zero otherwise.

Figure 3 indicates that there is less of an engine-placement effect during takeoff. In fact, for takeoffs, the three aircraft with two wing-mounted engines now appear slightly below the fit line. A small correction term e is thus subtracted from $t_1(\epsilon,B)$ for aircraft with two wing-mounted engines. Thus, the expression for the onset of decay for takeoffs is also a function of three variables and is given by:

$$t_1(\epsilon,B,E)=[0.70+0.11(\log(1/\epsilon)-1)] B + 5 \log(1/\epsilon) + 10 - eE, \qquad (14)$$

where

$$e = 2 \log_{10}(1/\epsilon) \qquad (15)$$

and E is one for two wing-mounted engines and zero otherwise. The corrected fitted values are plotted as asterisks in Figures 2 and 3.

21

Note that this method of dealing with the effect of two-wing-mounted engines is somewhat inconsistent, in that the baseline fits to the data (Eqs. 10 and 11) should have excluded the aircraft with two wing-mounted engines.

Reference 1 plotted an analysis similar to that in Figure 2 as a log-log plot. The slope of such a plot gives the power law dependence of decay time on aircraft wingspan. Figures 4 and 5 show the data of Figures 2 and 3 replotted on log-log scales. The landing relationship in Figure 4 is not as consistent as that shown in Figure 34 of Reference 4, which showed a slope of 0.34 between log decay time and log wingspan.

The lines fitted to the data in Figures 4 and 5 were drawn through the B-727 and B-747 data points. The resulting lines are roughly consistent with the data points for all aircraft of the non-two-wing-mounted-engines category except the DC-9, which shows considerably longer decay onsets. The slopes in Figure 4 (landing) range from 0.48 (ε=0.001) to 0.50 (ε=0.10). These values are larger than noted in Reference 2, but would be reduced to about the same value if the lines were drawn midway between the DC-9 and B-727 data points.

The slopes in Figure 5 (takeoff) are considerably larger, ranging from 0.83 (ε=0.10) to 1.00 (ε=0.001). Note that, the takeoff results are close to being consistent with the common assumption of linear aerodynamic scaling, where the vortex decay distance is proportional to the wingspan.
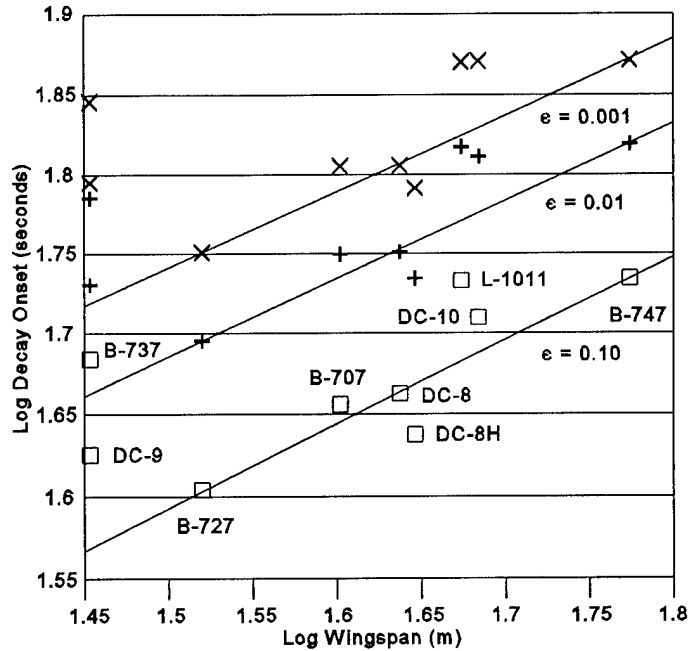
Figure 4. Decay Onset for Landing Data
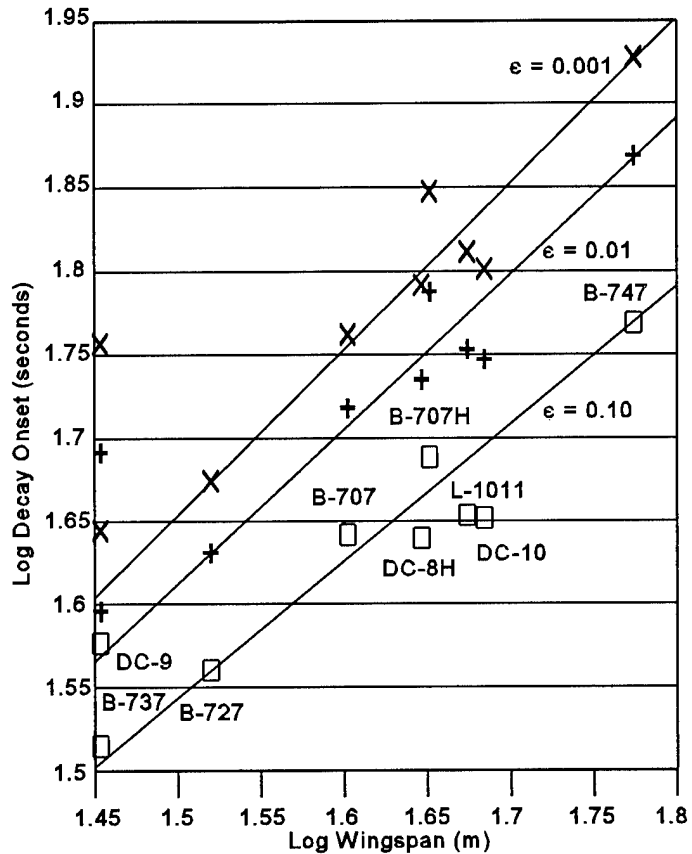
Figure 5. Decay Onset for Takeoff Data

22

2.3 MODEL LIMITATIONS

2.3.1 Hazard Model Additions

The following issues require further work to improve and validate the vortex encounter hazard model:

1) The current model is based on a static view of a wake vortex encounter and does not directly consider:

   a) The pilot response time, and

   b) The aircraft response time (moment of inertia effect).

   The current model attempts to reduce the parameter f to account for the dynamics of a wake vortex encounter. Pilots have indicated that the hazard is related to the maximum roll angle induced by the encounter, which is related to aircraft and pilot response, as well as the vortex-induced torque. A more complete model must attempt to estimate the maximum roll angle. The influence of the various model parameters must be validated with flight tests.

2) The model must consider the effect of the encountering aircraft on the vortex. Any momentum or angular momentum imparted to the aircraft must be subtracted from the vortex and hence will reduce the force of the vortex winds on the wing.

3) The model must treat the vortex core more realistically. The effect of the high velocities in the vortex core are reduced by:

   a) The momentum effects mentioned in 2),

   b) Stall at high angles of attack (However, since stall takes time to develop, momentum effects are likely more important.), and

   c) The presence of the fuselage.

Considerable work has been done recently[16] by NASA on these issues.

2.3.2 Vortex Decay Model Additions

The vortex decay models can be improved by incorporating additional data and by improving the analysis methods.

2.3.2.1 Additional Data

The most significant limitations of the vortex decay models are related to limitations in the MAVSS data used to generate them. The following additional measurements would improve the usefulness of the decay models:

23

1) The MAVSS data were collected during normal daytime working hours. A complete model requires data from around the clock. The limited measurements collected in 1991 at Dallas/Fort Worth airport are a step in the right direction.

2) Many new aircraft types and models have been introduced into service since the last major MAVSS data collection effort (1980). Limited data were collected on the current aircraft fleet in 1990 and 1991, but additional data will be needed to provide a statistically valid description of vortex decay from the new aircraft types and models.

3) A basic assumption of the MAVSS analysis for longitudinal aircraft spacings is that the decay of Vortex 2 is equivalent to that of stalled vortices, which cannot be measured with the MAVSS as currently configured. This assumption could be validated by comparing the decay of stalled vortices to those moving slowly, but fast enough to pass two MAVSS antennas. This analysis requires statistically significant amounts of decay data for wake vortices stalled on the runway centerline. Currently, the most feasible method for collecting such data is to combine an array of ground-based anemometers, which can now[17] estimate vortex circulation for vortices close to the ground, with MAVSS antennas, which can determine[18] the height of stalled vortices.

2.3.2.2 Additional Analyses

The following analyses could be used to improve the vortex decay models:

1) The limited 1990 and 1991 MAVSS data should be incorporated into the existing vortex models.

2) The vortex decay analysis presented in Section 2.2.3.2 was completely independent of the analysis of Reference 1 and produced somewhat different results, which may be related to the different choice of parameters (decay power of 1.5 rather than 2.0, averaging radius of 20 m rather than 10 m). Both analyses were carried out on minicomputers using software no longer available. As part of the effort to incorporate new data into the vortex decay analysis, it would be worthwhile to reanalyze the O'Hare landing and takeoff data using current hardware and software.

3) The classification model would be improved if the data used only Vortex 2 to represent the decay of stalled vortices. The analysis could also be modified to better represent the differences between aircraft with two wing-mounted engines and those with other engine configurations.

3. SEPARATION ANALYSIS

This chapter makes use of the vortex decay model described in Section 2.2.2.

3.1 SAFE SEPARATION PROBABILITIES

The pre 1994 separations are assumed to be safe on the basis of no IFR wake-vortex accidents in 18 years when the standards and procedures are followed (see Section 1.6.1). Consequently, a "safe" hazard probability can be determined by looking at the hazard probabilities for the pre 1994 separation standards (Tables 1 and 3). Tables 10 and 11 show the vortex hazard probabilities at minimum separation (Table 3) for two values of the hazard parameter f, 1.0 and 0.5, respectively. The software listed in Appendix D was used to derive these probabilities. In the tables, values less than 10^{-6} are left blank since such low probabilities are not justified by the number of decay measurements (less than 500 Vortex 2 deaths for the B-727 and far fewer for other aircraft types). The B-707 and DC-8 vortex generators were divided into the Heavy and Large classes according to their radio calls. The following aircraft are specified by both weight class (Heavy, Large or Small) and wingspan b.

Tables 10 and 11 show how much the hazard probability can vary for different pairs of aircraft. The highest probabilities occur for 20-meter wingspan Large aircraft (e.g., Gulfstream II) behind the Large DC-8 and B-707 aircraft. However, this combination has occurred too infrequently in normal operations to constitute a reliable choice for a safe vortex hazard probability. The next highest probability in the tables occurs for a 30-meter wingspan aircraft following a Large DC-8. Since this size follower represents the DC-9 and the B-737, this combination has occurred often enough in normal operations to represent a high level of safety and hence a very safe hazard probability. The separation safety analysis will therefore consider a separation very safe if it leads to an equal or smaller hazard probability, i.e., 0.0020 for f = 1.0 or 0.13 for f = 0.5.

Since the current separation standards may be overly conservative, it is not possible to assess whether hazard probabilities higher than the value for a DC-9 behind a DC-8L are actually dangerous. Nevertheless, the safety level can be graded according to the hazard probability. Probabilities equal to or lower than the DC-9/DC-8L values would be considered highly safe, i.e., a safety level of "A." Probabilities comparable to the 20-meter Large aircraft behind a DC-8L represent a lesser level of safety, which will be assigned a safety level of "C." Probabilities in between these values would be graded safety level "B." Probabilities significantly higher than the C level would be graded safety level "D" or perhaps "F." These levels will be used in interpreting the results of the following examples. The probabilities used to define the hazard levels "A" and "C" are marked as ≡A and ≡C in Tables 10 and 11. All other probabilities in Tables 10 and 11 attain safety level "A" level except for the value for 20-meter Large aircraft behind the B-707, which is safety level "B."

Although the relative hazards for the different aircraft pairs do not depend upon the value selected for f, the probabilities for f = 0.5 vary so little between A and C safety levels (0.13 vs. 0.23) that the analysis method is not very convincing. The f = 0.5 analysis also suffers from

Table 10. Hazard Probability at Minimum Separation for $f = 1.0$

Leading Aircraft	Following Aircraft						
	Heavy		Large			Small	
	b=50m	b=40m	b=40m	b=30m	b=20m	b=20m	b=10m
Heavy							
B-747	3.1×10^{-6}	2.4×10^{-5}					
L-1011		1.1×10^{-5}			1.8×10^{-5}		
DC-10							
B-707H							
DC-8H							
Large							
DC-8	1.8×10^{-5}	2.5×10^{-4}	2.5×10^{-4}	2.0×10^{-3} ≡A	1.0×10^{-2} ≡C	2.2×10^{-5}	2.2×10^{-4}
B-707		2.5×10^{-5}	2.5×10^{-5}	3.0×10^{-4}	5.2×10^{-3} B	5.0×10^{-6}	8.4×10^{-5}
B-727				1.2×10^{-5}	4.8×10^{-4}		
B-737				4.5×10^{-6}	3.0×10^{-4}		
DC-9					8.9×10^{-5}		

Table 11. Hazard Probability at Minimum Separation for $f = 0.5$

Leading Aircraft	Following Aircraft						
	Heavy		Large			Small	
	b=50m	b=40m	b=40m	b=30m	b=20m	b=20m	b=10m
Heavy							
B-747	1.1×10^{-2}	2.3×10^{-2}	1.0×10^{-4}	4.3×10^{-4}	1.8×10^{-3}	1.8×10^{-4}	6.6×10^{-4}
L-1011	7.7×10^{-3}	1.9×10^{-2}	6.5×10^{-5}	3.8×10^{-4}	3.3×10^{-3}	4.1×10^{-4}	3.1×10^{-4}
DC-10	1.9×10^{-3}	5.7×10^{-3}	4.4×10^{-6}	4.4×10^{-6}	9.6×10^{-4}	7.8×10^{-5}	8.7×10^{-4}
B-707H	3.9×10^{-4}	2.3×10^{-3}		4.0×10^{-5}	5.9×10^{-4}	4.1×10^{-5}	1.3×10^{-3}
DC-8H	3.9×10^{-5}	3.1×10^{-4}			3.3×10^{-6}		
Large							
DC-8	3.1×10^{-2}	6.7×10^{-2}	6.7×10^{-2}	1.3×10^{-1} ≡A	2.3×10^{-1} ≡C	2.2×10^{-2}	5.4×10^{-2}
B-707	1.3×10^{-2}	3.4×10^{-2}	3.4×10^{-2}	6.9×10^{-2}	1.8×10^{-1} B	1.3×10^{-2}	3.8×10^{-2}
B-727	2.0×10^{-3}	7.1×10^{-3}	7.1×10^{-3}	2.3×10^{-2}	8.1×10^{-2}	2.0×10^{-3}	5.1×10^{-3}
B-737	2.0×10^{-3}	7.4×10^{-3}	7.4×10^{-3}	2.7×10^{-2}	8.7×10^{-2}	2.4×10^{-3}	8.5×10^{-3}
DC-9	2.0×10^{-4}	1.1×10^{-3}	1.1×10^{-3}	1.4×10^{-2}	5.6×10^{-2}	8.7×10^{-4}	2.9×10^{-3}

the influence of the MAVSS vortex detection threshold, which is near the f =0.5 hazard threshold, particularly for small averaging radii.

3.2 HIGH-RESOLUTION SEPARATIONS

The practical application of the separation analysis in the next three sections will consider separation standards that are of coarse resolution (mile or half mile) so that they are compatible with manual air traffic control. An automated air traffic control system may permit the use of higher resolution separations. This section presents high-resolution results from the separation model. For a fixed probability, the vortex age dependence of the "safe" separation is readily derived from the argument of the error function in the simple stochastic model (see Appendix C).

3.2.1 Time Separations

Time separations are the natural output of the separation model and are appropriate for time-based automated separation systems. Figures 6 and 7 show the safe separations as a function of following aircraft wingspan for the ten generating aircraft of the separation model. Data points are omitted when the model is not valid (initial strength less than hazard threshold).
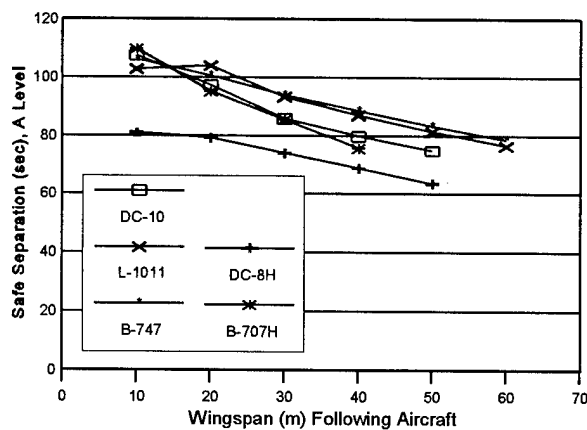
Figure 6. A-Level Safe Separation Behind Heavy Aircraft - Time
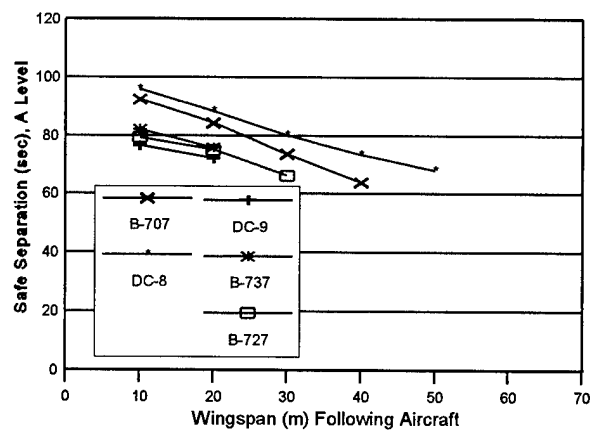
Figure 7. A-Level Safe Separation Behind Large Aircraft - Time

3.2.2 Distance Separations

Figures 8 and 9 show the distance separations corresponding to Figures 6 and 7. The assumed airspeed is 135 knots.

27
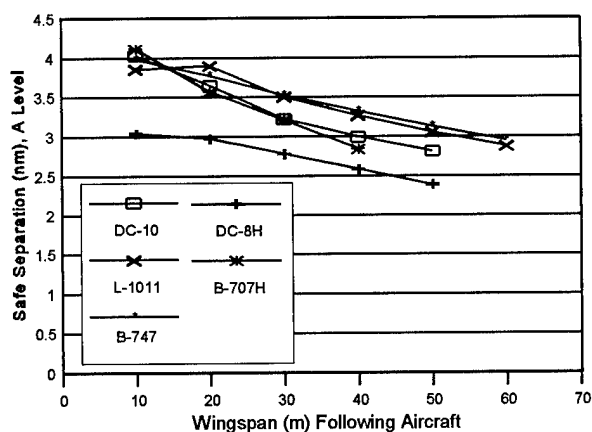
Figure 8. A-Level Safe Separation Behind Heavy Aircraft - Distance
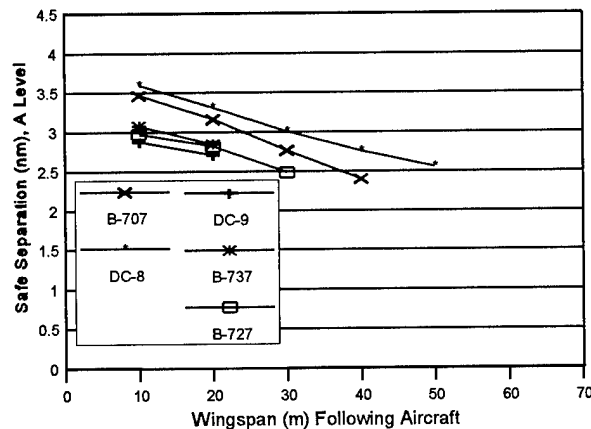
Figure 9. A-Level Safe Separation Behind Large Aircraft - Distance

3.3 2.5-MILE SEPARATION FOR SELECTED LARGE AND SMALL AIRCRAFT

In the mid 1980s, the FAA developed a special 2.5-mile separation standard (see Table 12) to be used at airports where the runway occupancy times are short enough to permit such separations. This separation was intended for Small aircraft and Large aircraft other than the B-757. Since the Large B-707 and DC-8 aircraft were no longer in service, the B-727 was the largest vortex generating aircraft subject to this separation.

Table 12. Special Wake Vortex IFR Separation Standards at Runway Threshold

Leading Aircraft Class	Following Aircraft Class				
	Heavy	Large	Large*	Small	Small*
Heavy	4 nm 107 sec	5 nm 133 sec	5 nm 133 sec	6 nm 160 sec	6 nm 160 sec
Large	3 nm 80 sec	3 nm 80 sec	3 nm 80 sec	4 nm 107 sec	4 nm 107 sec
Large*	3 nm 80 sec	3 nm 80 sec	2.5 nm 67 sec	4 nm 104 sec	4 nm 107 sec
Small	3 nm 80 sec	3 nm 80 sec	2.5 nm 67 sec	3 nm 80 sec	3 nm 80 sec
Small*	3 nm 80 sec	3 nm 80 sec	2.5 nm 67 sec	3 nm 80 sec	2.5 nm 67 sec

* Same size aircraft for short runway occupancy times (B-757 excluded).

Table 13 shows the hazard probabilities calculated for the DC-8, B-707, B-727, B-737 and DC-9 for 2.5 nm separation. The 30-meter wingspan aircraft following the last three aircraft easily meet the "A" level safe separation criterion developed above. Thus, B-737 and DC-9 aircraft would be expected to safely follow the B-727 and other B-737s and DC-9s at 2.5-mile separation. The hazard probabilities for 20-meter wingspan aircraft behind these three aircraft are at the B or C level of safety. Finally, the 10-meter wingspan aircraft following the B-727 or B-737 has a D level of safety. Note that all three aircraft sizes have safety levels of C or below behind the B-707 and DC-8 at 2.5 miles; such pairs are therefore unlikely candidates for reduced separation.

Table 13. Vortex Hazard Probabilities and Safety Levels for 2.5 Nautical Mile Separations

Leading Aircraft	Following Aircraft		
	b = 30 m	b = 20 m	b = 10 m
f = 1.0	Hazard Prob. A = 0.0020, C = 0.010		
DC-8	0.026 D	0.073 F	0.14 F
B-707	0.0074 C	0.047 D	0.11 F
B-727	0.00087 A	0.010 C	0.021 D
B-737	0.00028 A	0.0058 B	0.015 D
DC-9	0.000080 A	0.0027 B	0.0096 C
f = 0.5	Hazard Prob. A = 0.13, C = 0.23		
DC-8	0.33 D	0.45 F	0.55 F
B-707	0.23 C	0.39 D	0.50 F
B-727	0.12 A	0.25 C	0.31 D
B-737	0.13 A	0.26 C	0.35 D
DC-9	0.085 A	0.20 C	0.27 C

3.4 THREE-MILE SEPARATION FOR HEAVY AIRCRAFT

The safe Heavy-Heavy separation is determined by the smallest Heavy aircraft following the largest Heavy (B-747). The aircraft at the bottom end of the Heavy class (B-767, DC-8H) have wingspans in the range of 40 to 50 meters. The hazard probabilities for these aircraft behind a B-747 at three nautical miles are shown in Table 14 and are all above the "A" level probability. The 50-meter wingspan followers have a "B" level of safety and the 40-meter wingspan followers have a "C" level of safety. The B-747 (b = 60 m), however, has an "A" safety level behind another B-747 at three miles. This result suggests that some benefit might be obtained by dividing the Heavy class into two classes, as is discussed in the next section.

Table 14. Three-Nautical-Mile Hazard Probability and Safety Level Behind the B-747

b (m)	f = 1.0	f = 0.5
60	0.0013 A	0.12 A
50	0.0041 B	0.17 B
40	0.011 C	0.23 C

3.5 SUPERHEAVY CLASS

Aircraft larger than the B-747 are now on the drawing boards and may be introduced into service in the near future. Table 15 shows how the aircraft classification weight limits might appear if a Superheavy class, including the B-747 and larger aircraft, were to be defined. Table 16 presents proposed separations for the classes in Table 15. The following features of Table 16 should be noted:

1) Current separations are unchanged for all leading aircraft except those assigned to the new Heavy class (DC-10, L-1011, B-767), for which all following separations have been reduced by one mile. This reduction should improve the landing capacity at airports where these aircraft operate.

2) Table 16 presents separations that satisfy the difference rule, namely that the separation between two classes should be equal to $a + b\Delta$, where Δ is the class number difference. In this case a is 3 and b is 1. Such a difference rule should reduce[19] air traffic controller workload.

Table 15. Proposed New Wake Vortex Aircraft Classes: MCGTOW Limits

Wake Vortex Class	Lower Weight Limit (lbs)	Upper Weight Limit (lbs)
Small	0	12,499
Large	12,500	300,000
Heavy	301,000	600,000
Super-heavy	601,000	none

The safety analyses for Superheavy and Large leading aircraft are included in earlier tables. The aircraft following the B-747 at the distances in Table 16 have an "A" safety level [see Table 14 for a following B-747 (b=60m) and Tables 10 and 11 for other following aircraft]. Separations for aircraft following the Large class are unchanged; the hazard probabilities are therefore given in Tables 10 and 11. All are "A" level except 20-meter Large aircraft behind the B-707 and DC-8, which remain "B" and "C," respectively.

Table 16. Wake Vortex IFR Separation Standards with Superheavy Class

Leading Aircraft Class	Following Aircraft Class			
	Superheavy	Heavy	Large	Small
Superheavy	3 nm, 107 sec	4 nm, 107 sec	5 nm, 133 sec	6 nm, 160 sec
Heavy	3 nm, 80 sec	3 nm, 80 sec	4 nm, 107 sec	5 nm, 160 sec
Large	3 nm, 80 sec	3 nm, 80 sec	3 nm, 80 sec	4 nm, 107 sec
Small	3 nm, 80 sec	3 nm, 80 sec	3 nm, 80 sec	3 nm, 80 sec

Table 17 shows the results of the safety analysis for aircraft following the new Heavy aircraft, where the separations have been reduced by one mile. All have safety level "A" except for Heavy aircraft with 40-meter wingspan, where the safety level is "B" or "C."

Table 18 provides a complete picture of the safety analysis (f =1.00) for the four-class separation standards defined in Tables 15 and 16. This separation rule results in safety level "A" for all cases

Table 17. Hazard Probability behind Heavy Aircraft for Table 16 Separations

Leading Aircraft	Following Aircraft						
	Heavy (3 nm)		Large (4 nm)			Small (5 nm)	
	b=50m	b=40m	b=40m	b=30m	b=20m	b=20m	b=10m
Heavy	$f = 1.00$						
L-1011	1.5×10^{-3} A	6.6×10^{-3} B	1.1×10^{-6} A	1.0×10^{-4} A	1.3×10^{-3} A	1.8×10^{-7} A	1.1×10^{-7} A
DC-10	2.5×10^{-4} A	1.5×10^{-3} A	4.7×10^{-7} A	8.1×10^{-6} A	2.9×10^{-4} A	8.3×10^{-8} A	6.4×10^{-7} A
Heavy	$f = 0.50$						
L1011	1.5×10^{-1} A-	2.1×10^{-1} C	1.9×10^{-2} A	4.2×10^{-2} A	1.1×10^{-1} A	3.3×10^{-3} A	2.7×10^{-3} A
DC-10	7.9×10^{-2} A	1.3×10^{-1} A	5.7×10^{-3} A	1.6×10^{-2} A	6.2×10^{-2} A	9.6×10^{-4} A	5.9×10^{-3} A

Table 18. Hazard Probability at Possible New Minimum Separation Rule for $f = 1.0$.

Leading Aircraft	Following Aircraft							
	Super-heavy	Heavy		Large			Small	
	b=60m	b=50m	b=40m	b=40m	b=30m	b=20m	b=20m	b=10m
Super-heavy								
B-747	1.3×10^{-3}	3.1×10^{-6}	2.4×10^{-5}					
Heavy								
L-1011	2.4×10^{-4}	1.5×10^{-3}	6.6×10^{-3} B	1.1×10^{-5}	1.0×10^{-4}	1.3×10^{-3}		
DC-10	2.8×10^{-5}	2.5×10^{-4}	1.5×10^{-3}		8.1×10^{-6}	2.9×10^{-4}		
B-707H		1.3×10^{-5}	3.3×10^{-4}		6.8×10^{-6}	1.7×10^{-4}		1.6×10^{-6}
DC-8H		2.0×10^{-6}	4.5×10^{-5}					
Large								
DC-8		1.8×10^{-5}	2.5×10^{-4}	2.5×10^{-4}	2.0×10^{-3} ≡A	1.0×10^{-2} ≡C	2.2×10^{-5}	2.2×10^{-4}
B-707			2.5×10^{-5}	2.5×10^{-5}	3.0×10^{-4}	5.2×10^{-3} B	5.0×10^{-6}	8.4×10^{-5}
B-727					1.2×10^{-5}	4.8×10^{-4}		
B-737					4.5×10^{-6}	3.0×10^{-4}		
DC-9						8.9×10^{-5}		

except two, which lie on the boundaries between classes: 40-m Heavy aircraft behind the L1011 and 20-m Large aircraft behind the DC-8 and B-707. These boundaries could be adjusted by reducing the B-767 to Large and all aircraft smaller than the DC-9 and B-737 to Small. The available data on the wakes of the current Large aircraft smaller than the DC-9 and B-737 have not been analyzed; consequently, it is difficult to judge the safety of the new, broader Small class that would result from this change. More data are needed also for the B-757 and B-767, which now occupy the boundary between the Large and Heavy classes.

4. ALTERNATIVE SEPARATION ANALYSIS

The analyses presented in this chapter are based on the alternative separation model presented in Section 2.4.2.

4.1 SAFE SEPARATION MODEL

The software for calculating the hazard probabilities for the alternative separation model is listed in Appendix E. Since the probabilities are similar to those presented in the tables of Chapter 3, the actual probabilities will not be presented here. Instead, only the resulting safe separation distances are presented (as in Section 3.2.2). Then results are presented in Figures 10-13 for both "A" and "C" levels of safety. The wingspan b dependence of the safe separation is simpler for this model than for the original model because b enters the hazard model equation (Equation 4) only through the parameter b on the right hand side and not through the limiting circulation value Γ'_T on the left; Γ'_T is independent of b for this model.

In order to compare the safe separation model used in this analysis with those derived by other methods, it is useful to specify a power law relationship of safe separation distance D to the wingspans of the leading (B) and following (b) aircraft:

$$D = G \ B^m / b^q, \qquad (16)$$

where G is a constant and m and q are the powers defining the dependence upon the wingspans of the leading and following aircraft, respectively.

The simple stochastic model assumes that, after a certain delay, a vortex decays inversely with the square of vortex age. This decay results in a safe separation model where the safe separation distance is inversely proportional to the square root of the follower wingspan, i.e., q=0.5.
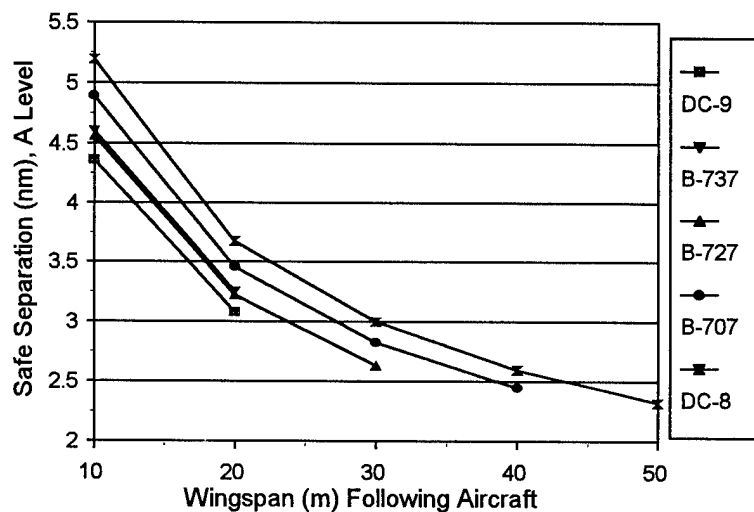
Figure 10. A-Level Safe Separation Behind Large Aircraft
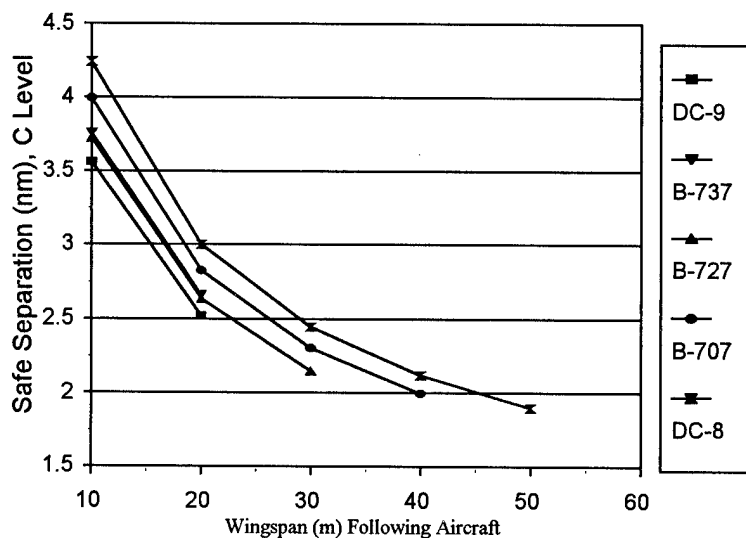
Figure 11. C-Level Safe Separation Behind Large Aircraft

33

The dependence of the safe separation distance on the wingspan of the generating aircraft is illustrated in Figures 14 and 15 which shows how the safe separation for a 20-meter span following aircraft depends upon the span of the generating aircraft for A and C levels of safety, respectively. The lines in the plots are for a power m = 0.5 and a DC-8 safe separation of 3.9 and 3.1 miles for A and C levels of safety, respectively. They give a rough indication of how the safe separation depends upon leader wingspan; however, a power law does not give a good fit to the points for individual aircraft types. Note that the lines in Figures 14 and 15 give a safe separation S that depends upon the span ratio (B/b) between leader and follower; D is proportional to the square root of the span ratio.

As noted in other analyses of the O'Hare landing data, Figures 14 and 15 indicate that, for the same wingspan, a relatively greater separation is needed following aircraft with two wing-mounted engines (B-737, L-1011 and DC-10).

4.2 AIRCRAFT CLASSIFICATION

4.2.1 Approach

The classification approach consists of two steps:

1) Define the list of classes and the desired separation matrix. Note that
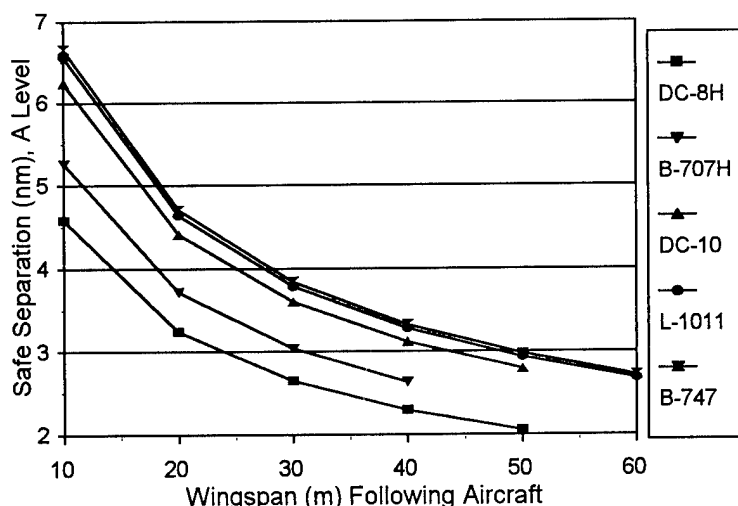
Figure 12. A-Level Safe Separation Behind Heavy Aircraft
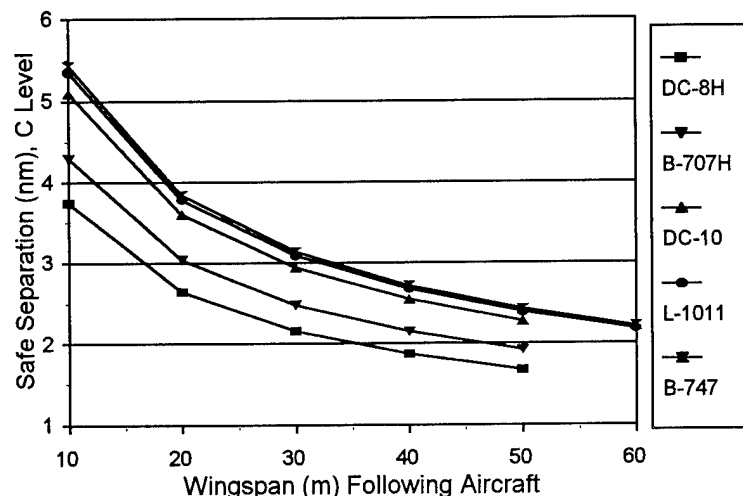
Figure 13. C-Level Safe Separation Behind Heavy Aircraft
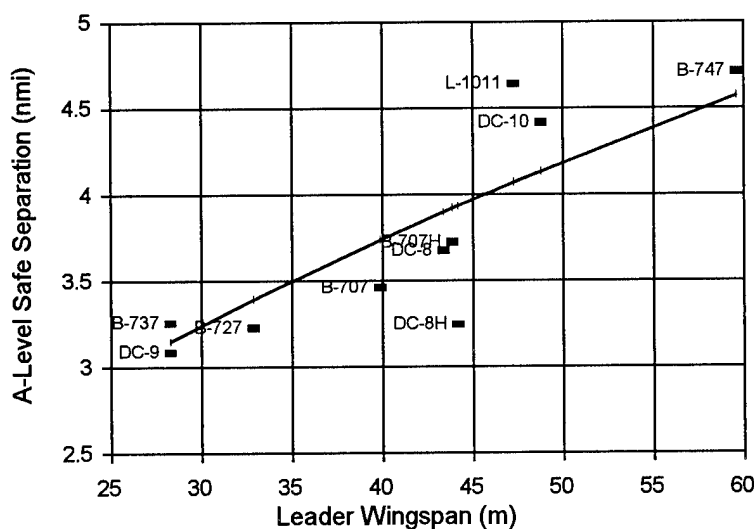
Figure 14. A-Level Safe Separation for 20-m Span Follower vs. Leader Wingspan

34

controller workload will be reduced if the separation distance between two classes depends upon the number of classes in between[19].

2) Select the aircraft to be assigned to the different classes. Use the safe separation curves in Figures 10-13 to determine the wingspan boundaries between classes. These boundaries need to be consistent with the original assignment of aircraft to classes.
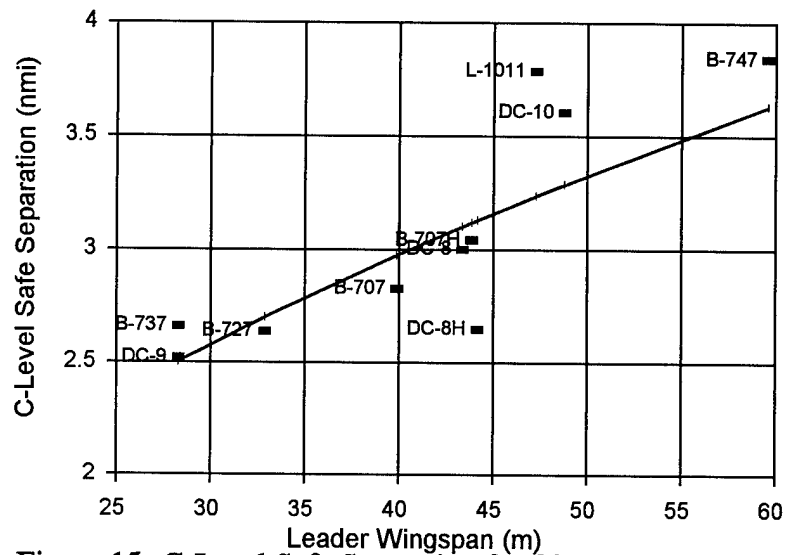
Figure 15. C-Level Safe Separation for 20-m Span Follower vs. Leader Wingspan

Table 19. Class Definitions

Class	Symbol	Comment
Heavy	H	B-747 is biggest member
Large	L	DC-8/B-707H defines upper boundary B-737/DC-9 defines lower boundary
Medium	M	Lower boundary from analysis
Small	S	Lower boundary from analysis
Super Small	SS	Too small for Small class

Table 19 lists the classes needed to cover the range of operating aircraft for this analysis. Table 20 shows the separation matrix selected for an A level of safety. Table 21 shows the separation matrix selected for a C level of safety.

Table 20. A-Level Safety Separation Matrix

Leader Class	Follower Class				
	H	L	M	S	SS
H	3	4	5	6	7
L	2.5	3	4	5	6
M		2.5	3	4	5
S			2.5	3	4
SS				2.5	3

Table 21. C-Level Safety Separation Matrix

Leader Class	Follower Class				
	H	L	M	S	SS
H	2.5	3	4	5	6
L		2.5	3	4	5
M			2.5	3	4
S				2.5	3
SS					2.5

35

4.2.2 Results

Tables 22 and 23 present the results of the separation analysis for A and C levels of safety, respectively. The B-747 safe separations are used to represent the Heavy class as leader. The very similar B-707H and DC-8 safe separations are used to represent the Large class as leader and may well represent the B-757, which is the biggest current aircraft in the pre 1994 Large class. The analysis gives consistent span breakpoints for following aircraft behind both the Large and Heavy classes. Surprisingly, both the A and C levels of safety also define the same span breakpoints between following classes; the C-level of safety reduces the separations by one increment compared to the A-level of safety. The follower span breakpoints must be consistent

Table 22. Follower Class Separations and Span Limits for A-Level Safety

Leader Class		Follower Class								
		H	b limit H-L	L	b limit L-M	M	b limit M-S	S	b limit S-SS	SS
		Sep.		Sep.		Sep.		Sep.		Sep.
H	B-747	3	49 m	4	28 m	5	19 m	6	13 m	7
L	B-707H DC-8	2.5	45 m	3	30 m ≡A	4	18 m	5	12 m	6

Table 23. Follower Class Separations and Span Limits for C-Level Safety

Leader Class		Follower Class								
		H	b limit H-L	L	b limit L-M	M	b limit M-S	S	b limit S-SS	SS
		Sep.		Sep.		Sep.		Sep.		Sep.
H	B-747	2.5	46 m	3	33 m	4	19 m	5	12 m	6
L	B-707H DC-8			2.5	30 m	3	20 m ≡C	4	12 m	5

with the assumed leader class assignments:

H-L   The pre 1994 wingspan break between the Large and Heavy classes is 38 meters (B-757) to 44 meters (A-310). Keeping the A-310 in the Heavy class is reasonably consistent with the range of break points (45-49 m) in Tables 4 and 5.

L-M   Keeping the B-737/DC-9 (span = 28 meters) in the Large class is consistent with the A-level safety analysis, considering that they defined the A-level of safety (the A-level definition at 30-meter span was an approximation). The C-level safety analysis calls for a L-M break as high as 33 meters (behind Heavies); 28 meters is probably close enough considering the uncertainties in the analysis.

M-S   The 19-meter break point is reasonably consistent.

36

S-SS   The 12-meter break point is consistent. Whether there are enough aircraft below this limit to make a separate class is open to question.

4.2.3 Conclusions

The classification analysis based on the Chicago O'Hare MAVSS landing data leads to the following conclusions:

1) The same-class separation is 2.5 miles for C-level safety and 3 miles for A-level safety.

2) The pre 1994 Large class is divided into a Large and Medium class where the lower end of the new Large class is the small jet transport (B-737, DC-9, F-100). The new Large class separation behind the Heavy class is reduced from the current 5 miles to 4 miles (A-level safety) or 3 miles (C-level of safety). For A-level safety the Medium class separation behind the Heavy class is unchanged at 5 miles, but the separation behind the new Large class in increased from 3 to 4 miles. Conversely, for C-level safety the Medium class separation is kept at 3 miles behind the Large class but decreased from 5 to 4 miles behind the Heavy class.

3) The new Small class (span of 12 to 19 meters) includes some aircraft formerly classified as Large because their maximum certificated gross takeoff weight is above 12,500 lbs. The old Small class has separations of 6 miles behind Heavies and 4 miles behind Larges. The A-level separations for the new Small class are similar, with the addition of an intermediate separation of 5 miles behind the Medium class. The C-level separations are significantly reduced, being 5 miles behind Heavies, 4 miles behind Mediums and 3 miles behind Larges.

4) A new Super Small class for aircraft with spans less than 12 meters may or may not be needed.

Note that these conclusions are subject to the limitations of the MAVSS data, which were discussed in Section 2.3.2.

4.3 FOUR-CLASS SYSTEM

The Wake Turbulence Industry Team proposed a four-class system with somewhat optional class limits. The FAA Wake Vortex Program Office reviewed the proposal and selected the specific limits shown in Table 24. This section evaluates the safety of these separations. Section 1.5.2 illustrated the reasons for changing the classification criterion from weight to wingspan.

4.3.1 Safety Criteria

The following criteria were used in the safety evaluation (in descending order of emphasis):

- Observed safety of 1976-1994 IFR separations: No vortex-related accidents when standards followed.

- Observed IFR incidents: UK encounter statistics; Appendix B relates encounter rate to follower/leader span ratio.

37

Table 24. Recommended Four-Class Limits and Separation Matrix

Class Wingspan Limits (ft)	Aircraft in Class		Leader Class	Follower Class			
	Lightest	Heaviest		H	L	M	S
>180	A-330	B-747-400	H	3	4	5	6
120-180	B-757	MD-11	L		3	4	5
60-120	DHC-6	B-727	M			3	4
<60	CE-172	Jetstar	S				3

- Observed VFR accidents: Citation and Westwind behind B-757 suggest a threat to high performance business jets, which (1) are susceptible to induced roll because of their short wingspans and (2) are fast enough to maintain close spacing behind jet transports.

- Wake vortex decay measurements: 1976-77 Chicago O'Hare landing measurements; Section 4.1 summarized the separation analysis.

Heavier weight is placed on operations since research efforts are not yet definitive. Heavier weight is placed on IFR than VFR since VFR problems are more efficiently addressed with vertical rather than longitudinal separations (see Section 1.5.1).

4.3.2 Separation Changes

Table 25 shows the relationship between the pre 1994 classes and recommended new classes. Special class codes (e.g., S1) are needed to define the changes in separation relative to the 1976-1994 separations, which are listed in Table 26.

Both reductions and increases in separation are noted in Table 26. Most of the reductions are for L leading aircraft and are a consequence of splitting the old H class and reducing the spacing

Table 25. Comparison of Old and New Aircraft Classes

Pre 1994	Class Code	New Class
Heavy	H	Heavy
	L	Large
Large	B-757	
	M	Medium
	S1	Small
Small	S2	

Table 26. Separation Changes from 1976-1994 Values

	Follower					
Leader	H	L	B-757	M	S1	S2
H	-1	0	-1	0	+1	0
L	-1	-1	-2	-1	0	-1
B-757	0	0	0	+1	+2	+1
M	0	0	0	0	+1	0
S1	0	0	0	0	0	-1
S2	0	0	0	0	0	0

38

behind the smaller members of the old H class. The separation increases are caused by (a) specifically increasing spacings behind the B-757 by grouping it with the smaller members of the old H class and (b) by moving the smaller members of the old L class into the new S class.

4.3.3 Safety Analysis

The separations will be analyzed by leader class:

H Leader:
    Smallest H follower at 3 miles:
        1)   Separation reduced by one mile from 1976-1994 value of four miles.
        2)   UK encounter rate analysis gives 2.56 miles equal-encounter-rate (EER) separation for the smallest H (B-747) behind the largest H (B-747-400).
        3)   O'Hare analysis gives 2.9-mile A-level safe separation for 180-foot (55-meter) span aircraft behind B-747.
    Reduction is supported.

    Smallest L (B-757) follower at 4 miles:
        1)   Apart from B-757, separation unchanged from 1976-1994. B-757 separation reduced by one mile from five to four miles.
        2)   UK encounter rate analysis gives 4.02 miles EER separation for the smallest L (B-757) behind the largest H (B-747-400). The resulting encounter rate is near the maximum observed in the UK.
        3)   O'Hare analysis gives 3.6-mile A-level safe separation for 120-foot (37-meter) span aircraft behind the B-747.
    Reduction for B-757 is reasonably well supported.

    Smallest M follower (19-meter span) at 5 miles:
        1)   No change from 1976-1994.
        2)   Not represented in UK statistics, but would have EER separation of 8.02 miles behind B-747-400 if functional dependence is valid for smaller following aircraft. Estimated encounter rate would be about 2.5 times highest UK level.
        3)   O'Hare analysis gives 4.9-mile A-level safe separation for 19-meter span aircraft behind the B-747.
    Supported by 1976-1994 history, O'Hare data. Extrapolation of UK encounter statistics not justified.

    Smallest S follower (11-meter span) at 6 miles:
        1)   No change from 1976-1994.
        2)   Not represented in UK statistics.
        3)   O'Hare analysis gives 6.4/5.2-mile A/C-level safe separation for 11-meter span aircraft behind the B-747.
    Supported by 1976-1994 history, O'Hare data at B-level (between A and C level).

L Leader:

Smallest L follower (B-757) at 3 miles:

1) Separation reduced by two miles from 1976-1994 value of five miles.

2) UK encounter rate analysis gives 3.22-mile EER separation for B-757 behind the largest H (MD-11). Estimated encounter rate would be about 200 per 100,000 queued landings, which is just above the highest observed in the UK.

3) O'Hare analysis gives 3.5/2.9-mile A/C-level safe separation for 120-foot span behind the L-1011 which is the L with greatest safe separation.

Reduction supported at maximum UK encounter rate and C-level O'Hare separation.

Smallest M Follower (19-meter span) at 4 miles:

1) Separation is reduced one mile from the 1976-1994 value of five miles.

2) Not represented in UK statistics, but would have EER separation of 6.42 miles behind MD-11 if functional dependence is valid for smaller following aircraft. Estimated encounter rate would be about 2.5 times highest UK level.

3) O'Hare analysis gives 4.9/4.0-miles A/C-level safe separations for 19-meter span behind the L-1011 which is the L with the greatest safe separation.

Some reduction supported by 1976-1994 operations since largest old H aircraft (B-747) is not in new L class and smaller aircraft in old L class have been moved to new S class. Supported by O'Hare data at C-level.

M Leader:

Smallest M follower (19-meter span) at 3 miles:

1) Same as in 1976-1994.

2) Not represented in UK statistics, but would have EER separation of 4.06 miles behind B-727 if functional dependence is valid for smaller following aircraft. Estimated encounter rate would be about 1.6 times highest UK level.

3) O'Hare analysis gives 3.4/2.5-miles A/C-level safe separations for 60-foot span behind the B-727.

Supported by 1976-1994 experience and O'Hare B-level safety.

Smallest S follower (11-meter span) at 4 miles:

1) Same as in 1976-1994.

2) Not represented in UK statistics.

3) O'Hare analysis gives 4.8/3.9-miles A/C-level safe separations for 11-meter span behind the B-727 which is the largest M.

Supported by 1976-1994 experience and O'Hare C-level safety.

S Leader:

    Smallest S follower (11-meter span) at 3 miles:

        1)   Spacing behind biggest S reduced by one mile from 1976-1994 value of four miles.

        2)   Not represented in UK statistics.

        3)   Not represented in O'Hare data.

        Some reduction supported by 1976-1994 operations since only smallest old L aircraft are in new S class.

The safety of the proposed four-class separations is better justified, both as leaders and as followers, for jet transport aircraft than for smaller aircraft. The lack of definitive information for the smaller aircraft suggests that more emphasis be placed on small aircraft in future wake vortex studies.

5. CLASSIFICATION ANALYSIS

In contrast to the separation analysis, presented in Section 3, which was limited to leading aircraft for which wake vortex data have been collected, the classification model developed in this section attempts to define where both new and existing aircraft fit into the pre 1994 classes and separation standards defined in Tables 1 and 4. An aircraft classification model accepts parameters describing a particular aircraft and outputs a classification such as Small, Large, or Heavy. The current classification model uses a single parameter, maximum certificated gross takeoff weight, to classify an aircraft for wake-vortex related separation standards. This section develops a classification model based upon both aircraft size and engine placement. The hazard model was described in Section 2.1.2 and the decay model in Section 2.2.4.

5.1 COMPUTATION OF HAZARD DISTANCES

The hazard model of Section 2.1.2 combined with the models for initial strength and vortex decay in Sections 2.2.4.1 and 2.2.4.2 provides an estimate of hazard distances for leader/follower aircraft combinations. These hazard distances can then be used to classify aircraft types. The algorithm for computing the hazard distance d_H for a given probability level and a given leader/follower pair consists of the following steps:

1)   Input all required parameters:

           W   Maximum gross landing weight of the leading aircraft
           B   Wingspan of the leading aircraft
           V   Landing speed of the leading aircraft
           E   Engine-placement flag to indicate if leader aircraft has two wing-mounted engines
           b   Wingspan of the following aircraft
           ϵ Hazard probability threshold.

2)   Compute characteristics of the vortices generated by the leading aircraft. These characteristics are the initial vortex strength $\Gamma_\infty(0)$ using Equation 7; the onset of vortex decay $t_1(\epsilon,B,E)$ using Equation 12 or 14; and the vortex core radius r_c where

$$r_C = (2.5/59.6)\,B \tag{16}$$

is defined as a fraction of the wingspan (based on B-747 LDV data[20]). Note that most jet transport aircraft wake vortices have a smaller relative core size than the B-747 wake vortex; therefore, this assumption could under estimate the encounter severity for small following aircraft.

3)   Compute the threshold value $\Gamma_{\infty T}$ for the total vortex strength Γ_∞ when the vortex is still considered hazardous to a following aircraft with wingspan b. A vortex with strength greater than or equal to $\Gamma_{\infty T}$ is considered hazardous; otherwise, the

43

vortex is not considered hazardous. A hazard exists (Equation 4) to a following aircraft if

$$\Gamma'(b/2) \geq 2.5 \, b \text{ (metric units)} \tag{17}$$

where b is the wingspan of the following aircraft and the roll-control fraction f is taken as 0.5. [This choice of f produces acceptable hazard probabilities (Table 11) within the measurement statistics for most aircraft types.] Substituting 2.5 b for $\Gamma'(r)$ in Equation 6 and solving for Γ_∞ yields the desired equation for the hazardous strength threshold:

$$\Gamma_{\infty T} = 2.5 \, b/[1-(2r_c/b)\tan^{-1}(b/2r_c)]. \tag{18}$$

4) Compute the time t_H required for the vortex strength to decay from its initial value $\Gamma_\infty(0)$ to its hazard threshold value $\Gamma_{\infty T}$. Using Equation 9 with the empirically derived value n = 1.5 for the decay rate yields the desired expression:

$$t_H = t_1[\Gamma_\infty(0)/\Gamma_{\infty T}]^{.667} \tag{19}$$

5) Compute the hazard distance d_H for the given leading/following aircraft combination. This distance is simply the groundspeed V of the leading aircraft times the hazard time t_H:

$$d_H = V \cdot t_H. \tag{20}$$

For landing operations the maximum aircraft landing speed is used [consistent with initial strength estimate, but perhaps not the best choice]. For takeoff operations, a fixed value of 75 meters per second (145 knots) is used. This value was obtained from the Volpe Center wake vortex database for Toronto takeoffs[21] which included groundspeeds. The average groundspeed was close to 75 meters per second for all the aircraft in the database.

5.2 RESULTS

The hazard distance algorithm was programmed and the results are presented for landing aircraft in Tables 27 and 28 and for departing aircraft in Tables 29 and 30. The hazard distances in most cases are slightly greater than the current separation standards which have proven safe over many years of operation. The greater distances therefore reflect the conservative assumptions underlying the models and are primarily useful for ranking the various aircraft according to their vortex hazard.

For both landings and takeoffs, the hazard distances were computed for hazard probability thresholds of $\epsilon = 0.10$ and 0.01. Of course, the hazard distances are greater at a one percent hazard probability threshold than at a ten percent hazard probability threshold. These threshold values were chosen because they are consistent with the number of operations used for most of

44

Table 27. Landing Classification Model: $\epsilon = 0.01$

Leading Aircraft Type	Model Parameters $\Gamma_\infty(0)$ (m²/s)	r_c (m)	t_1 (s)	b=	Following Aircraft Size 10 m Hazard Distance (nm)	20 m	30 m	40 m
B-737	212	1.2	59.0		6.2	4.4	3.5	3.0
DC-9	203	1.2	51.3		5.4	3.9	3.1	2.6
A-320	221	1.4	61.2		6.6	4.9	3.9	3.3
B-727	246	1.4	52.8		6.2	4.5	3.6	3.1
B-707	225	1.7	55.6		6.7	5.0	4.1	3.5
DC-8	236	1.8	56.9		6.2	4.8	3.9	3.3
B-757	267	1.6	62.8		7.9	5.9	4.8	4.1
B-707H	245	1.8	57.0		6.8	5.2	4.3	3.6
DC-8H	264	1.9	57.2		6.8	5.2	4.3	3.6
A-300	330	1.9	65.3		8.8	6.8	5.6	4.7
B-767	287	2.0	66.6		8.5	6.7	5.5	4.7
L-1011	366	2.0	66.4		10.3	8.0	6.6	5.6
DC-10	394	2.1	67.3		10.2	8.0	6.6	5.7
B-747	430	2.5	63.2		9.5	7.8	6.5	5.6

Table 28. Landing Classification Model: $\epsilon = 0.10$

Leading Aircraft Type	Model Parameters $\Gamma_\infty(0)$ (m²/s)	r_c (m)	t_1 (s)	b=	Following Aircraft Size 10 m Hazard Distance (nm)	20 m	30 m	40 m
B-737	212	1.2	47.0		4.9	3.5	2.8	2.4
DC-9	203	1.2	41.3		4.3	3.1	2.5	2.1
A-320	221	1.4	49.2		5.3	3.9	3.1	2.7
B-727	246	1.4	42.8		5.0	3.7	3.0	2.5
B-707	225	1.7	45.6		5.5	4.1	3.4	2.8
DC-8	236	1.8	46.9		5.1	3.9	3.2	2.7
B-757	267	1.6	50.8		6.4	4.8	3.9	3.3
B-707H	245	1.8	47.0		5.6	4.3	3.5	3.0
DC-8H	264	1.9	47.2		5.6	4.3	3.5	3.0
A-300	330	1.9	53.3		7.2	5.6	4.5	3.9
B-767	287	2.0	54.6		7.0	5.5	4.5	3.8
L-1011	366	2.0	54.4		8.4	6.6	5.4	4.6
DC-10	394	2.1	55.3		8.4	6.6	5.4	4.6
B-747	430	2.5	53.2		8.0	6.6	5.5	4.7

Table 29. Takeoff Classification Model: $\epsilon = 0.01$

Leading Aircraft Type	Model Parameters			b=	Following Aircraft Size			
	$\Gamma_\infty(0)$ (m²/s)	r_c (m)	t_1 (s)		10 m	20 m	30 m	40 m
					Hazard Distance (nm)			
B-737	212	1.2	38.9		5.1	3.6	2.9	2.4
DC-9	183	1.2	43.5		5.1	3.7	2.9	2.5
A-320	221	1.4	43.5		5.5	4.1	3.3	2.8
B-727	222	1.4	46.6		6.0	4.4	3.5	3.0
B-707	202	1.7	52.3		6.0	4.5	3.6	3.1
DC-8	212	1.8	55.2		6.3	4.8	3.9	3.3
B-757	267	1.6	46.8		6.5	4.9	3.9	3.4
B-707H	220	1.8	55.4		6.4	5.0	4.0	3.4
DC-8H	238	1.9	55.7		6.8	5.2	4.3	3.6
A-300	330	1.9	52.0		7.9	6.1	5.0	4.2
B-767	287	2.0	54.6		7.3	5.7	4.7	4.0
L-1011	366	2.0	54.3		8.6	6.7	5.5	4.7
DC-10	394	2.1	56.0		9.1	7.2	5.9	5.1
B-747	387	2.5	68.3		10.0	8.3	6.9	6.0

Table 30. Takeoff Classification Model: $\epsilon = 0.10$

Leading Aircraft Type	Model Parameters			b=	Following Aircraft Size			
	$\Gamma_\infty(0)$ (m²/s)	r_c (m)	t_1 (s)		10 m	20 m	30 m	40 m
					Hazard Distance (nm)			
B-737	212	1.2	32.8		4.3	3.1	2.4	2.1
DC-9	183	1.2	35.3		4.1	3.0	2.4	2.0
A-320	221	1.4	36.7		4.7	3.4	2.8	2.3
B-727	222	1.4	38.0		4.9	3.6	2.9	2.4
B-707	202	1.7	42.9		4.9	3.7	3.0	2.5
DC-8	212	1.8	45.4		5.2	4.0	3.2	2.8
B-757	267	1.6	39.6		5.5	4.1	3.3	2.8
B-707H	220	1.8	45.6		5.3	4.1	3.3	2.8
DC-8H	238	1.9	45.9		5.6	4.3	3.5	3.0
A-300	330	1.9	44.1		6.7	5.1	4.2	3.6
B-767	287	2.0	46.3		6.2	4.9	4.0	3.4
L-1011	366	2.0	46.1		7.3	5.7	4.7	4.0
DC-10	394	2.1	47.6		7.8	6.1	5.0	4.3
B-747	387	2.5	56.7		8.3	6.9	5.7	5.0

the empirical fits in this analysis. Typically, data for several hundred landings or takeoffs were available for most aircraft, so these probability thresholds do not extrapolate beyond the measured data. Also, these hazard probabilities are the same orders of magnitude as the hazard probabilities for many leader/follower combinations using the current minimum separations (see Table 11).

Within each table, the first column lists the type of aircraft generating the vortex. The aircraft are listed in order of increasing maximum landing weight. A horizontal line separates the aircraft classified as Large from those classified as Heavy, using the pre 1994 classifications of Table 1. The second column contains the initial vortex total strength $\Gamma_\infty(0)$. Columns three and four contain the calculated vortex core radius r_c and time t_1 of decay onset for probability threshold ϵ. The last four columns give hazard distances in nautical miles for following aircraft with wingspans of 10, 20, 30 and 40 meters, respectively.

5.3 CLASSIFICATION OF THE A-300, A-320, B-757, AND B-767 AIRCRAFT

The aircraft classification model can be applied to four aircraft for which statistical analyses of vortex data are not available. By comparing the hazard distances for these aircraft with the hazard distances for the other aircraft in Tables 27 to 30, it is generally possible to predict the proper class for the new aircraft, subject to the limitations of the models. The A-320 clearly belongs in the Large class and the A-300 and B-767 belong in the Heavy class.

The classification of the B-757 is more difficult because it is close to the Large/Heavy boundary. For landing operations, the hazard distances behind a B-757 are greater than the hazard distances behind both the B-707H and the DC-8H which are each currently classified as Heavy. On takeoff, the hazard distance behind the B-757 is comparable to the hazard distances behind the B-707H and the DC-8H. Note that two studies[2,4] have shown that all B-707 and DC-8 aircraft can be safely reclassified as Large. If the B-707H and DC-8H remain classified as Heavy, then this model would suggest that the B-757 should also be classified Heavy. If the B-707H and DC-8H aircraft were reclassified as Large, then the B-757 could define the top of the Large class or the bottom of the Heavy class.

47

6. DISCUSSION

The analyses of Chapters 2, 3 and 4 were carried out independently. Some of the results will be correlated in this chapter.

6.1 SEPARATION MODEL

The separation model of Reference 1 has been updated and used to examine a number of separation systems. The most promising is a four-class system (Section 3.5, Table 16) that adds a Superheavy class (Boeing 747 and larger aircraft) to the existing three classes (Heavy, Large and Small). According to the separation model, this system can probably be defined to reach an A level of safety for all aircraft pairs, although the sensitivity of the results to the core measurement limitations of the MAVSS were not studied. Since the four-class system reduces separations behind the new Heavy class, it would likely increase airport capacity. This separation also provides "class difference" separations[19] that should result in reduced controller workload.

6.2 ALTERNATIVE SEPARATION MODEL

The alternative separation model does not require any corrections for MAVSS core measurements and, consequently, the results are more robust. This model was used twice, in Section 4.2, Table 20, and in Section 4.3, Table 24, to study essentially the same four-class system studied with the separation model in Section 3.5, Table 16. However, the class names and the aircraft assigned are different for the three analyses. The final analysis in Section 3.5, Table 16, is the most complete since it considers *all* available criteria for assessing the safety of an aircraft classification and separation system.

6.3 CLASSIFICATION MODEL

The classification model was designed to classify all aircraft for both landing and takeoff. Three basic parameters: weight, wingspan and engine configuration (along with some airspeed assumptions), were used to characterize the vortex generating aircraft. One parameter, the wingspan, was used to characterize the encountering aircraft. The form of the classification model presented was a first effort which could be readily improved in its treatment of a number of model parameters. The classification model was akin to the alternative separation analysis is using total circulation to avoid the core measurement limitations of the MAVSS. However, it assumed that all aircraft have the same ratio of vortex core radius to wingspan as the B-747; this assumption is certainly not true and could lead to the same type of error for small aircraft as generated by the MAVSS core errors.

6.4 STATUS OF CALCULATED SAFE SEPARATIONS

The models presented in this report have not been validated to the point that their results can be used to assure the safety of new separation standards. The improvements outlined in Section 2.3 should eventually, however, permit modeling to approach this goal. Nevertheless, the results at the current level of model sophistication have identified a promising four-class separation option

for further study.

In the future, automated terminal area ATC systems (TATCA, CTAS) will remove the constraints on the number of allowed separation classes. Then separation models can be used to define minimum required separations for each pair of aircraft. Such fine-grained separations should improve capacity over the current standards which need to be safe for the largest member of the leading class and the smallest member of the following class and hence are overly conservative for most aircraft pairs.

6.5 DEFINITION OF THE HEAVY/LARGE BOUNDARY

Current separation standards treat the B-757 as a special aircraft splitting the Large/Heavy boundary. In effect, the B-757 is now the fourth class defined in the analyses of Chapter 4. The required separations behind the B-757 are intermediate to those required behind Large and Heavy aircraft. The analyses all suggest that additional aircraft from the lower end of the Heavy class could be safely added to the B-757 class. This reclassification would save some of the airport capacity now lost to current wake vortex separation standards.

APPENDIX A - HAZARD MODEL

During the 1970s, two remote sensing systems were developed and used successfully to measure aircraft wake vortices:

a) Monostatic Acoustic Vortex Sensing System (MAVSS) and

b) Laser Doppler Velocimeter (LDV).

Both of these systems are capable of measuring the tangential velocity of a wake vortex. In order to make use of such measurements to determine safe aircraft separations, the hazard to an encountering airplane must be related to the tangential velocity profile. A model for the hazard of a wake vortex encounter is needed to determine this relationship. Thus, a hazard model is an essential part of any analysis of wake-vortex data which attempts to define the operational limits set by the wake-vortex hazard.

The basic assumption of the Volpe hazard model is that the primary wake-vortex hazard to an encountering airplane is related to the loss of roll control during an axial vortex penetration. This assumption ignores other possible hazards such as structural damage, engine flameout or loss of control surface effectiveness. The next assumption of the model is that the wake vortex hazard depends only upon the ratio of the roll induced on the wings of the airplane by the vortex to the maximum roll control (i.e., full roll input by the pilot) capability of the airplane. The fundamental parameter of the model is f, the ratio of the maximum controllable vortex-induced roll to the maximum roll control. This hazard definition ignores both the dynamics of the encounter (e.g., such issues as pilot response time, duration of the encounter, geometry of the encounter, etc.), the altitude of the encounter which determines how long the pilot has to make his recovery from the upset, and other flight conditions (such as IFR/VFR considerations, etc). If the pilot's response were instantaneous, he could control his airplane as long as the induced roll is less than his roll control authority (i.e., the value of f would be 1.00). The model accounts approximately for all response lag effects by adopting a value of f significantly less than 1.00. Although the value of f is uncertain, an analysis using the hazard model can still be reliable if the results are insensitive to the value selected for f.

This appendix presents the Volpe Center vortex encounter hazard model as it was understood in the mid 1980s. It does not, for example, reflect the considerable work done by NASA since that time. The hazard model was first formulated in Reference 9 where it was used, in conjunction with MAVSS data, to develop a hazard probability model for wake vortices out of ground effect. One of the assumptions of this formulation turned out to be unrealistic and it was reformulated in Reference 2. In Reference 20, the basic mathematical assumption of the model was refined to give a small correction factor. Reference 1 examined the wingspan dependence of the hazard model and considered a wider range of model parameters. All of the hazard model information from these separate documents will be consolidated here to make the model more easily understood and to encourage further improvements in the model.

51

A.1 BASIC MODEL

The goal of the basic model is to relate the vortex-induced rolling moment on the wing of the encountering airplane to the strength of a wake vortex. The basic mathematical assumption can be justified by two approximations:

a) The force on the wing is given by strip theory, and

b) The wing is uniform in cross section along its length.

According to strip theory, the force F(y) on a particular wing strip at distance y from the airplane centerline is given by:

$$F(y) = v(y) \, K(y), \qquad (A-1)$$

where v(y) is the vertical component of the wind at position y and K(y) is the ratio between the force and the vertical wind. The model assumes that K(y) is independent of y. Within strip theory, constant K(y) follows from the assumption of a uniform untwisted wing cross section and a linear dependence in lift coefficient upon angle of attack (i.e., no stall). For constant K(y) = K the torque on a wing of span b becomes:

$$T = K \int_{-b/2}^{b/2} v(y) \, y \, dy. \qquad (A-2)$$

Studies have shown that the largest torque occurs when the wing is centered in the wake vortex, as illustrated in Figure 16. Thus, Equation A-2 can be modified by changing the span variable y to the vortex radius r and by substituting the definition of the vortex circulation profile $\Gamma(r) \equiv 2\pi \, r \, v(r)$:
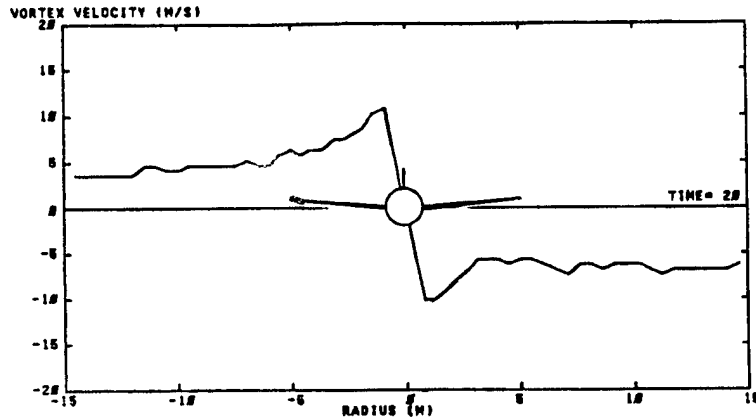

Figure 16. Worst Case Vortex Encounter

$$T = (K/2\pi) \int_{-b/2}^{b/2} \Gamma(r) \, dr = (Kb/2\pi) \, \Gamma(b/2), \qquad (A-3)$$

where the average circulation $\Gamma(r)$ up to radius r is defined by the equation:

$$\Gamma(r) = (1/2r) \int_{-r}^{r} \Gamma(r') \, dr'. \qquad (A-4)$$

52

Since the term "vortex strength" is sometimes applied to the circulation $\Gamma(r)$, in particular the limiting value Γ_∞ as r approaches infinity, $\Gamma'(r)$ will often be referred to as the "average strength". The average strength defined by Equation A-4 is well suited for analyzing experimental data for two reasons:

a) The averaging process reduces the effect of random velocity measurement errors.

b) In contrast to theoretical vortex velocity profiles where the vortex radius r is never negative, experimental measurements usually include both sides of a vortex and hence are directly equivalent to Equation A-2. Averaging the two sides of a vortex eliminates, to zero order, the systematic error caused by the velocity field of the ambient wind and the other vortex.

The notable feature of Equation A-3 is that the torque depends only upon the average circulation, but not on the shape of the velocity profile producing the average circulation. This independence of the velocity profile can be used in a mathematical trick to relate the average vortex strength to the maximum roll control of the encountering airplane.

Suppose the airplane is rolling at rate p (radians/second) with the roll control at its limit. Next suppose that the wing is imbedded in a wake vortex with a solid body rotation in the opposite direction from the roll that is just large enough to cancel the roll of the airplane. The net effect is that the pilot can just control the airplane in such a vortex. The strength of this wake vortex is therefore the hazard threshold corresponding to $f = 1.00$. The velocity profile for solid body rotation at angular rate p is given by $v(r) = pr$. This velocity can be integrated by Equation A-4 to give the hazard threshold:

$$\Gamma'_T(b/2) = (\pi/6)pb^2. \tag{A-5}$$

It is useful to express the maximum roll rate p of the encountering airplane as the nondimensional parameter $\hat{p}$:

$$\hat{p} = pb/2V, \tag{A-6}$$

where V is the airspeed of the airplane. The nondimensional roll rate $\hat{p}$ is typically 0.06 for commercial airplanes and 0.08 for general aviation airplanes. With this substitution, Equation A-5 becomes:

$$\Gamma'_T(b/2) = (\pi/3)fbV\hat{p}, \tag{A-7}$$

where the factor f has been added to give the hazard threshold for other values of f. Equation A-5 is for $f = 1.00$. Much of the data analysis using the hazard model used the expression:

$$\Gamma'_T(b/2) \approx 5fb \quad (m^2/s), \tag{A-8}$$

which is consistent with the nominal values for landing jet transport airplanes (V = 130 knots (68 m/s) and $\hat{p} = 0.07$). The exact expression of Equation A-7 should be used when the product $V\hat{p}$ is significantly different from these values.

The wingspan dependence of the wake-vortex average strength hazard threshold can be derived from Equation A-7 by dividing by b/2 to place all the wingspan factors on the left side of the

equation:

$$\Gamma'_T(b/2)/(b/2) = H_T \equiv (2\pi/3)fV\hat{p}. \tag{A-9}$$

The left side of Equation A-9 can be evaluated using what has been termed the "simple" vortex model:

$$\Gamma(r) = \Gamma_\infty/[1 + (r_c/r)^2] \tag{A-10}$$

where r_c is the vortex core radius. Combining Equations A-10 and 2 leads to the corresponding tangential velocity equation:

$$v(r) = (r\,\Gamma_\infty/2\pi)/[r^2 + r_c^2] \tag{A-11}$$

The integral of Equation A-4 can be carried out analytically for Equation A-10 to yield:

$$\Gamma'(r) = \Gamma_\infty[1 - (r_c/r)\tan^{-1}(r/r_c)]. \tag{A-12}$$

Substituting Equation A-12 into Equation A-9 gives the vortex hazard as a function of wingspan, as shown in Figure 17. The range of wingspans experiencing a hazard from a particular vortex is critically dependent on the value of H_T calculated in Equation A-9. The value H_{T1} in Figure 17 gives no hazardous wingspans. The value H_{T2} yields a hazard for wingspans between 2 r_c and 5.2 r_c. Reducing H_{T2} by a factor of two to H_{T3} drastically increases the hazard wingspan range to 0.69 r_c through 14.8 r_c. For further reductions in H_T the lower hazard bound will decrease proportionally to H_T and the upper bound inversely with H_T.

The fact that a given vortex is safe for both small and large wingspans may be surprising at first glance, but it can be readily understood by careful examination. For large wingspans the vortex velocities are too small over much of the wingspan to present a hazard. (Moreover, the effect of
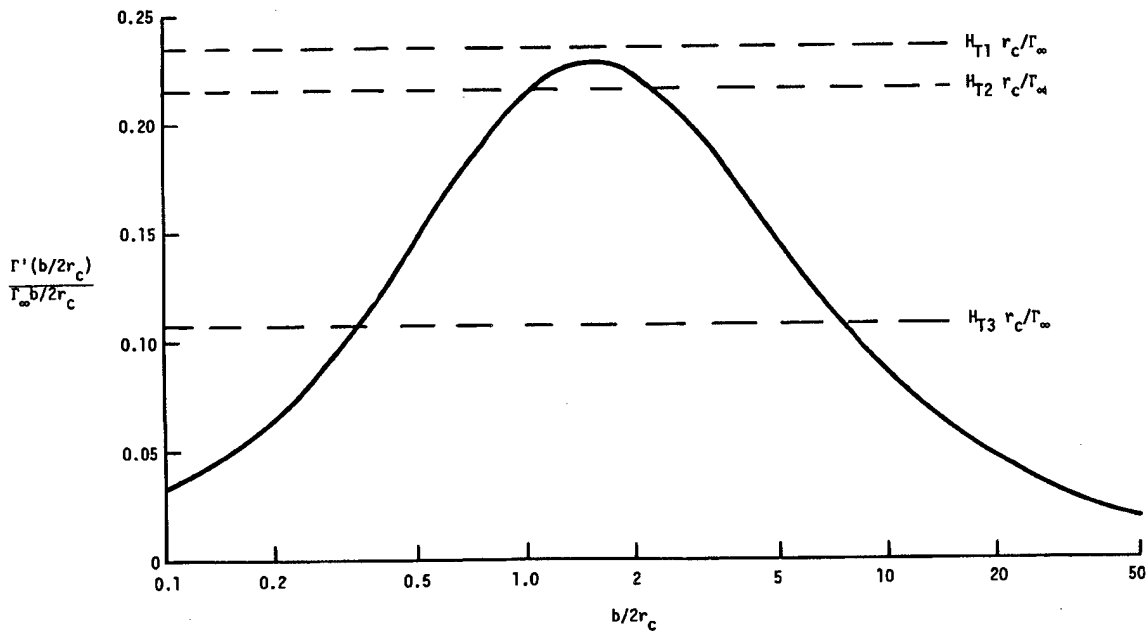

Figure 17. Wingspan Dependence of Vortex Hazard

54

the other vortex, which is more or less ignored in the model, will reduce the hazard.) For wingspans smaller than the core size, the encountering airplane experiences only the local velocity gradient in the core and not the full velocity variation of the vortex.

A.2 REFINEMENTS

The assumptions of the basic model were examined in Reference 20 by using vortex lattice theory[22] to calculate the rolling moment induced on the encountering airplane by a wake vortex. This theory assumes no stall along the wing, but otherwise properly treats the effect of wing planform and variation of vortex velocity v(y) along the wing. The calculations divided the wing into four chordwise panels and eight spanwise panels on a semispan. Increasing the number of spanwise panels to 16 produced only a small change in the results (a decrease of 2 to 4 percent in rolling moment). The vortex velocities are entered into the calculations as a variable angle of attack α along the wing:

$$\alpha(y) = v(y). \qquad (A-13)$$

The goal of the calculations was to assess the validity of using the average circulation Γ' (Equation A-3) to estimate the maximum rolling moment induced on a wing. The first calculations thus used the most extreme variations in velocity with the same value of $\Gamma'(b/2)$. The velocity profiles shown in Figure 18b were used: 1) inverse radius velocity (ideal line vortex), 2) constant velocity, and 3) linear velocity (as used for the derivation of the hazard model). [The curves in Figure 18 are labeled with these three velocity profiles.] These profiles are all for the same average circulation of 100 m²/s.
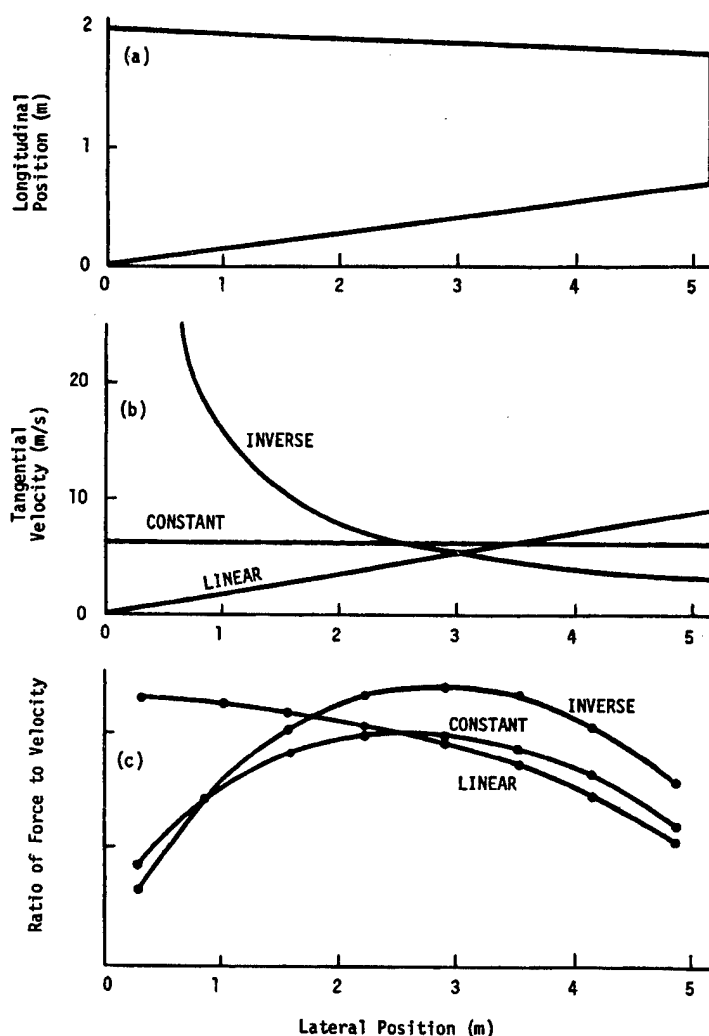

Figure 18. T-37 Rolling Moment Calculation: (a) Wing Planform, (b) Vortex Tangential Velocity, (c) Ratio of Force to Velocity

55

Table 31. Rolling Moment Coefficients for Average Vortex Circulation = 100 m²/s

AIRPLANE	WINGSPAN (m)	VELOCITY PROFILE		
		r⁻¹	Constant	r
T-37	10.3	0.0746	0.0663	0.0609
DC-9 (no flaps)	28.4	0.0297	0.0245	0.0114
DC-9 (flaps)	28.4	0.0264	0.0216	0.0187

The results of these calculations are shown in Table 31 which contains the vortex-induced rolling moment coefficient for two airplane types (T-37 and DC-9) at an airspeed of 70 m/s (136 knots). Figure 18a shows the wing planform for the T-37. Figure 18c shows the ratio of force to velocity (K(y) in Equation A-1) for the three velocity profiles (this function was assumed to be constant in the derivation of the hazard model). The DC-9 was evaluated with and without flaps extended. The flaps reduced the rolling moment coefficient by 12 percent.

The results in Figure 18 and Table 31 are for vortices with zero core radius. Using the more reasonable model vortex velocity profile of Equation A-11, Figure 19 shows how the vortex-induced rolling moment depends upon the vortex core radius. The rolling moment or torque is expressed in terms of C_{lv}, the vortex-induced torque coefficient, which is akin to the wing's lift coefficieint C_L. The values for constant and linear velocities are also shown for comparison. The model value for $r_c = 0$ corresponds to an inverse-radius velocity profile. The DC-9 values are with flaps extended.

The results of the rolling moment calculations show that average circulation, Γ'', can be used to give a reliable estimate of rolling moment coefficient according to the expression:

$$Q\ (\Gamma''/\Gamma''_{REF})\ (V_{REF}/V),\qquad (A-14)$$

where Q is a constant depending upon the airplane planform and wingspan and Γ''_{REF} and V_{REF} are the reference average circulation (100 m²/s) and airspeed (70 m/s) of the calculation. Values of Q were selected to evaluate B-747 data in Reference 20. The value of Q was particularly easy to select for the T-37 since in Figure 19 the same value is obtained for constant velocity (alleviated vortex) and r_c =
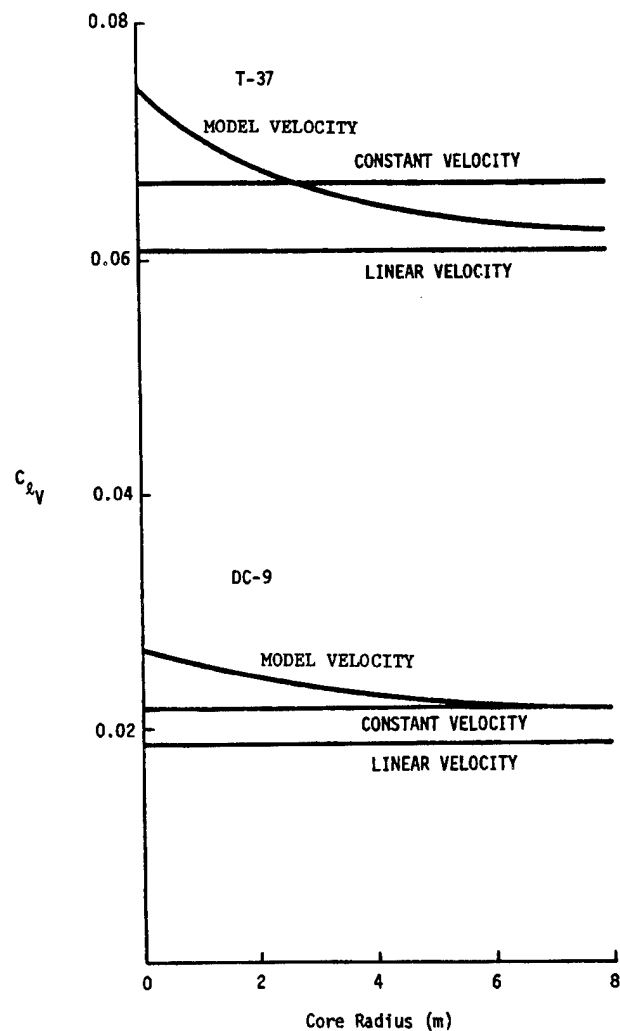

Figure 19. Vortex-Induced Rolling Moment Coefficient versus Vortex Core Radius for Average Circulation = 100 m²/s

56

2.5 (non-alleviated vortex). The value for the DC-9 was taken as $Q = 0.022$, the value for $r_c = 4$ m, which is a compromise between the alleviated and non-alleviated vortices. In either case, the errors in selecting Q are less than the experimental errors in measuring the average circulation Γ.

The results of the rolling moment calculations can be used to correct Equations A-7 through A-9 by a factor K which accounts for the planform and velocity profile effects. For example, Equation A-9 would become:

$$H_T = (2\pi/3)KfVp. \qquad (A-15)$$

The derivation of the hazard model is exact for a linear velocity profile. The correction factor K is therefore the ratio of the induced rolling moment produced by the linear velocity profile to that for the particular planform and velocity profile of concern for the same value of Γ. Figure 18 shows that, for constant Γ, the other profiles give larger induced rolling moments than the linear profile by a small percent. Consequently, the factor K is somewhat less than unity. Table 32 shows the values of K for the T-37 and the DC-9 for four different velocity profiles.

Table 32. Correction Factors

Airplane	T-37	DC-9
Wingspan (m)	10.3	28.4
Correction Factor K		
Const. Vel.	0.92	0.87
$r_c=0$	0.82	0.71
$r_c=2.5m$	0.91	0.78
$r_c=5m$	0.95	0.85

A.3 HAZARD PARAMETER

The exact value of the parameter f has not been determined. The wake-vortex encounter simulation studies of the 1970s were not directed to find a reliable value for f, but were designed to answer other questions, such as:

a) How close can one fly safely to a strong wake vortex? Answer: about 30 meters from the center.

b) What parameter of a wake-vortex upset best represents the hazard perceived by the pilot? Answer: the upset bank angle[12,23].

c) How does the wake-vortex upset hazard depend upon altitude and VFR versus IFR? Answer: Larger upsets are acceptable at higher altitudes[10,24].

It should be noted that the variations noted in c) imply that a fixed value of f is unrealistic and that f should depend upon altitude, visibility and ceiling.

The value $f = 0.5$ has been used in many analyses and is based on two observations. During the 1979 alleviation testing at the NASA Dryden Flight Research Center (Reference 20) measurements were on the amount of roll control inputs used by pilots flying a T-37 airplane into the B-747 wake. Under conditions where the pilots reported "no rotary motion in the wake," they were using about half the roll control capability of the T-37. At one time Earl Hastings of the NASA Langley Research Center carried out numerical simulations on wake-vortex encounters just before landing. For one run where the airplane just avoided crashing, the vortex strength corresponded to $f = 0.4$. It should be noted that one virtue of the selection $f = 0.5$ is that it represents about the lowest vortex strength that can be measured by the MAVSS (Reference 2).

A.4 MODEL USE

As mentioned above, some care must be used in applying the vortex hazard model in a data analysis. Any analysis where the results depend strongly upon the value selected for f cannot be trusted because the value of f is so uncertain. In principle, one should select f = 0.5 and examine the results as f is varied between 0.25 and 1.00. In practice, the range of variation of f for experimental vortex data is limited by the sensitivity of the sensor used to collect the data. It does not make sense to extend the sensitivity analysis to a region where the data are invalid.

Although it would appear that uncertainty in the value of f would severely limit the utility of the hazard model, nevertheless, many important questions can be addressed. For example, analyses in Chapters 3 and 4 have no dependence upon the value of f. The unimportance of the exact value of f stems from the probabilistic nature of vortex decay. The uncertainty in f is compensated by the uncertainty in how low the vortex hazard probability must be to declare an aircraft separation system safe. In fact, it is much easier to declare the current separation system safe, based on many years operational experience, than to define a safe vortex hazard probability. The probability of a hazardous vortex encounter depends upon too many parameters to be well defined.

It should be noted that the hazard model assumes an isolated wake vortex. If the wingspan of the encountering airplane is larger than twice the spacing between a pair of wake vortices, the hazard is reduced by the effect of the other vortex.

A.5 NEEDED IMPROVEMENTS

The vortex hazard model makes many simplifying assumptions that could be improved to make the model more accurate. In particular, the following items would appear to affect the hazard parameter f:

a)   Altitude,
b)   VFR/IFR,
c)   Airplane wingspan,
d)   Airplane/pilot response time,
e)   Turbulence level (which can mask the initial pilot perception of a vortex encounter), and
f)   The impact[25] of the encountering aircraft on the vortex.

References 23-25 represent efforts which could help better define the variation in f. However, the basic concept of f ignores the dynamics of the encounter. A better understanding of the vortex encounter is needed. One approach toward assessing encounter dynamics would be to use a 6-degree of freedom encounter model to answer the following two questions:

a)   What is the worst encounter direction for a vortex encounter?

b)   How weak must a vortex be to make such a "worst case" encounter safe?

A better understanding of vortex encounter dynamics is also needed to address several other factors affecting the encounter hazard:

a)   Vortex distortion (e.g., via the Crow instability)

b)   Vortex inclination, and

c)   Vortex spacing

APPENDIX B - ANALYSIS OF UK ENCOUNTERS, 1982-1990

The analysis[8] of UK encounter statistics depends upon two assumptions:

The **first assumption** of the analysis is that the equal-encounter-rate (EER) separation D behind an aircraft depends upon the wingspan ratio B/b of the leading aircraft to the following aircraft. The factor for normalizing D is selected to give a separation of five miles for the DC-9 behind the B-747 (Table 33 shows the matrix of D for jet transport aircraft) :

$$D=5(B/59.6)(28.0/b) \qquad\qquad (B-1)$$

The **second assumption** of the analysis is that the encounter rate R depends upon the ratio of the EER separation D to the actual separation A (which is equal to the separation standard for the queued arrivals used to calculate the UK encounter rates):

$$R=F(D/A) \qquad\qquad (B-2)$$

Figure 20 shows that the function F(D/A) in Equation B-2 is well represented by a straight line for all high encounter rate data. The equal-encounter-rate given in Figure 20 for D/A = 1 is 175 per 100,000 queued landings, which is approximately the highest observed in the UK (DC-9 behind B-747). The DC-9 behind B-757 rate is slightly higher at 190 per 100,000 queued landings.

Table 33 and Figure 20 can be used to estimate the encounter rate for any pair of aircraft. For example, if the DC-9 separation behind the B-757 is increased from the EER value of 3.18 miles to 5 miles, the incident rate will drop to zero.
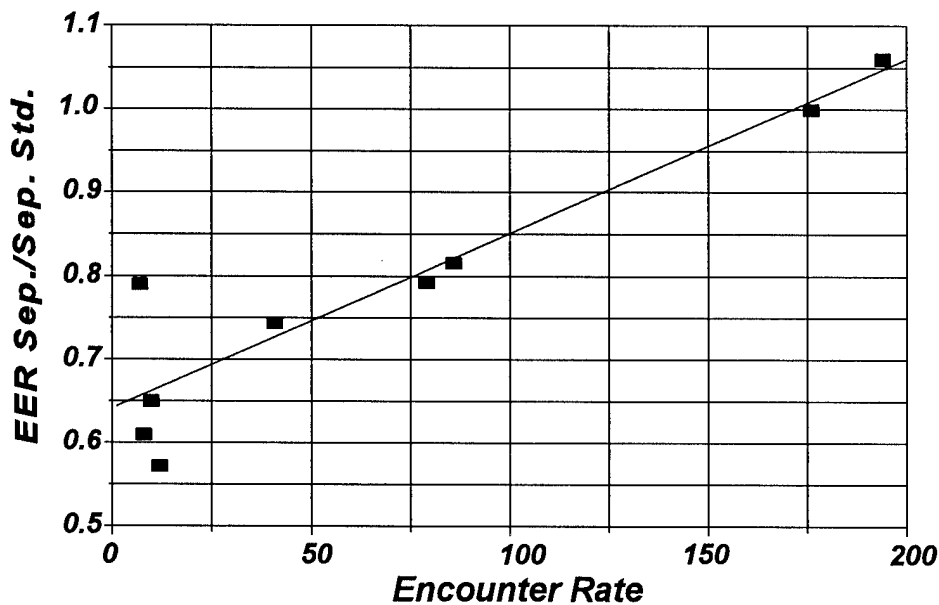

Figure 20. Relationship Between Encounter Rate and Ratio of EER Separation to Separation Standard

61

Table 33. Equal-Encounter-Rate Separation Matrix using Wingspan Ratio of Leader to Follower (Span in meters)

| | | Follower | | | | | | | | | | | | | | | | | | |
Leader	Span	B-747-4 64.92	B-777 60.93	A-340 60.30	B-747 59.60	MD-11 52.00	DC-10 50.40	DC-10 47.30	L-1011 50.00	L-1011 47.30	B-767 47.60	A300 44.80	A310 43.90	B-757 37.90	B-727 32.90	A320 33.91	MD-80 32.87	B-737 28.30	DC-9 28.00	F-100 28.08
B-747-400	64.92	2.35	2.50	2.53	2.56	2.93	3.03	3.22	3.05	3.22	3.20	3.40	3.47	4.02	4.64	4.50	4.64	5.39	5.45	5.43
B-777	60.93	2.20	2.35	2.37	2.40	2.75	2.84	3.03	2.86	3.03	3.01	3.19	3.26	3.78	4.35	4.22	4.35	5.06	5.11	5.10
A-340	60.30	2.18	2.32	2.35	2.38	2.72	2.81	2.99	2.83	2.99	2.98	3.16	3.23	3.74	4.31	4.18	4.31	5.01	5.06	5.04
B-747	59.60	2.16	2.30	2.32	2.35	2.69	2.78	2.96	2.80	2.96	2.94	3.13	3.19	3.69	4.26	4.13	4.26	4.95	5.00	4.99
MD-11	52.00	1.88	2.00	2.03	2.05	2.35	2.42	2.58	2.44	2.58	2.57	2.73	2.78	3.22	3.71	3.60	3.72	4.32	4.36	4.35
DC-10	50.40	1.82	1.94	1.96	1.99	2.28	2.35	2.50	2.37	2.50	2.49	2.64	2.70	3.12	3.60	3.49	3.60	4.18	4.23	4.22
DC-10	47.30	1.71	1.82	1.84	1.86	2.14	2.20	2.35	2.22	2.35	2.33	2.48	2.53	2.93	3.38	3.28	3.38	3.93	3.97	3.96
L-1011	50.00	1.81	1.93	1.95	1.97	2.26	2.33	2.48	2.35	2.48	2.47	2.62	2.68	3.10	3.57	3.46	3.57	4.15	4.19	4.18
L-1011	47.30	1.71	1.82	1.84	1.86	2.14	2.20	2.35	2.22	2.35	2.33	2.48	2.53	2.93	3.38	3.28	3.38	3.93	3.97	3.96
B-767	47.60	1.72	1.84	1.85	1.88	2.15	2.22	2.36	2.24	2.36	2.35	2.50	2.55	2.95	3.40	3.30	3.40	3.95	3.99	3.98
A300	44.80	1.62	1.73	1.75	1.77	2.02	2.09	2.22	2.10	2.22	2.21	2.35	2.40	2.78	3.20	3.10	3.20	3.72	3.76	3.75
A310	43.90	1.59	1.69	1.71	1.73	1.98	2.05	2.18	2.06	2.18	2.17	2.30	2.35	2.72	3.13	3.04	3.14	3.64	3.68	3.67
B-757	37.90	1.37	1.46	1.48	1.49	1.71	1.77	1.88	1.78	1.88	1.87	1.99	2.03	2.35	2.71	2.63	2.71	3.15	3.18	3.17
B-727	32.90	1.19	1.27	1.28	1.30	1.49	1.53	1.63	1.55	1.63	1.62	1.73	1.76	2.04	2.35	2.28	2.35	2.73	2.76	2.75
A320	33.91	1.23	1.31	1.32	1.34	1.53	1.58	1.68	1.59	1.68	1.67	1.78	1.81	2.10	2.42	2.35	2.42	2.81	2.84	2.84
MD-80	32.87	1.19	1.27	1.28	1.30	1.48	1.53	1.63	1.54	1.63	1.62	1.72	1.76	2.04	2.35	2.28	2.35	2.73	2.76	2.75
B-737	28.30	1.02	1.09	1.10	1.12	1.28	1.32	1.41	1.33	1.41	1.40	1.48	1.51	1.75	2.02	1.96	2.02	2.35	2.37	2.37
DC-9	28.00	1.01	1.08	1.09	1.10	1.26	1.30	1.39	1.32	1.39	1.38	1.47	1.50	1.74	2.00	1.94	2.00	2.32	2.35	2.34
F-100	28.08	1.02	1.08	1.09	1.11	1.27	1.31	1.39	1.32	1.39	1.39	1.47	1.50	1.74	2.00	1.95	2.01	2.33	2.36	2.35

APPENDIX C - SUMMARY OF VORTEX DECAY MODELS

The many vortex decay models of Reference 1 can be confusing. This appendix outlines the models and points out some errors in the original report.

The basic function of the models is the fraction $F(\Gamma_T, t)$ of wake vortices for which the average vortex circulation Γ (Equation 1) remains above the value Γ_T at vortex age t. [Note that Reference 1 on page 3-1 incorrectly specifies a vortex strength less than Γ_T.] For a following aircraft of wingspan b, the average circulation must be evaluated at radius b/2.

Simple Analytical Model

For old vortices the vortex decay data approximately fit the form (Reference 1, page 3-5, Equation 8):

$$F(\Gamma_T, t) = \exp[-\alpha(t^2 - d)]. \tag{C-1}$$

This equation is the basis for the simple analytical model outlined in Section B.1 of Reference 1. [Note that Equation 22 should read: $\alpha = G \Gamma_T$.]

Stochastic Model

The stochastic model is outlined in Section B.2 of Reference 1. It is based on a first assumption that the vortex strength is constant for a time t_1:

$$\Gamma = \Gamma_0 \qquad \text{for } t < t_1 \tag{C-2}$$

and then decays with a power n law:

$$\Gamma = \Gamma_0 (t_1/t)^n \quad \text{for } t > t_1. \tag{C-3}$$

[These are Equations 8 and 9 of this report.] Γ_0 is the initial vortex strength. The second assumption of the model is that t_1 has a normal distribution with mean value t_0 and standard deviation σ. Vortex decay is thus governed by three parameters: n, t_0 and σ. The resulting decay fraction is:

$$F(\Gamma_T, t) = \{1 - \text{erf}[(t_{1T} - t_0)/\sigma\sqrt{2}]\}, \tag{C-4}$$

$$t_{1T} = t (\Gamma_T/\Gamma_0)^{1/n}, \tag{C-5}$$

where erf is the error function. The three parameters of the model are determined by a least-square fit to the measured decay data. The value for n was usually fixed at 2, which gave the best fit for the B-747. The aircraft dependence on vortex decay (including both Vortex 1 and Vortex 2) (plotted in Figure 34 of Reference 1 on log-log scales) was determined by calculating the time for which a calculated fraction F =0.2, 0.02 and 0.002 of the vortices had not yet started to decay (for n = 2 and averaging radius 10 meters). [Note that the rightmost plots in Figure 35 of Reference 1 are for wind > 10 knots.]

Simple Stochastic Model

The stochastic model has too many parameters to give a well defined relationship between aircraft type and vortex decay. The simple stochastic model reduces the number of parameters by

assuming $t_0 = 3 \sigma$. It also accounts for the spread in initial vortex strength Γ_0 by assuming the measured mean value has a normal distribution with σ equal to 20% of Γ_0. The values of σ resulting from this fit to the decay data are plotted in Figure 40 of Reference 1 [with Vortex 1 and Vortex 2 labels reversed] as a function of averaging radius.

APPENDIX D - SEPARATION MODEL SOFTWARE

The following software listings implement the current version of the separation model. The simple stochastic model is used. The model parameters from Reference 1 (σ for Vortex 2 and averaging radii of 5, 10, 15, and 20 meters from Figure 40; Γ_0 from Table 9 for averaging radii 5, 10 and 20 meters) are coded into the main program. The σ value for 20-meter averaging radius is used for 25- and 30-meter averaging radii. The Γ_0 values for 15-, 25- and 30-meter averaging radii are obtained by fitting the "simple" vortex model to the 10- and 20-meter values.

```
C    HAZPRO.FOR is the main program.
C
C    CALCULATES THE WAKE-VORTEX HAZARD PROBABILITY FOR
C    FOLLOWING AIRCRAFT OF WINGSPANS 10,20,30,40,50,60 M.
C    FOR VARIOUS GENERATING AIRCRAFT
C
     DIMENSION AC(10),SSPAN(6),SPAN(6),SIG(6,10),GAM(6,10)
     DIMENSION PR(6),TIM(5),RC(10)
     CHARACTER*6 AC
     DATA AC/'DC-9','B-737','B-727','B-707','DC-8','DC-8H'
    A,'B-707H','DC-10','L-1011','B-747'/
     DATA SIG/13.0,12.8,12.2,11.4,11.4,11.4
    A,14.5,13.4,12.8,12.6,12.6,12.6
    A,12.4,12.0,11.4,11.3,11.3,11.3
    B,12.6,12.4,11.9,12.1,12.1,12.1
    B,12.6,12.3,12.2,12.2,12.2,12.2
    C,10.7,11.0,11.3,11.5,11.5,11.5
    C,14.6,13.4,13.5,13.2,13.2,13.2
    D,16.7,14.2,13.2,13.1,13.1,13.1
    D,15.0,14.7,14.0,14.0,14.0,14.0
    E,13.8,12.8,12.4,12.4,12.4,12.4/
     DATA GAM/51.,93.,0.,136.,0.,0.
    A,47.,94:,0.,138.,0.,0.
    A,60.,115.,0.,169.,0.,0.
    B,79.,136.,0.,188.,0.,0.
    B,85.,151.,0.,213.,0.,0.
    C,84.,152.,0.,210.,0.,0.
    C,83.,148.,0.,193.,0.,0.
    D,61.,138.,0.,218.,0.,0.
    D,69.,147.,0.,227.,0.,0.
    E,87.,181.,0.,299.,0.,0./
     DATA SSPAN,SPAN/5.,10.,15.,20.,25.,30.
    A,10.,20.,30.,40.,50.,60./
     DATA TIM/67.,80.,107.,144.,160./
        DATA RC/4.8,4.8,4.8,4.0,4.2
    A,4.0,3.2,5.8,5.5,6.3/
C
```

```
      DO 100 IA=1,10
C      Use 20-m Average Circulation as reference to get 15,25,30-m values.
      B=20.
      R=RC(IA)
      FB=1.-(R/B)*ATAN(B/R)
      A=15.
      FA=1.-(R/A)*ATAN(A/R)
      GAM(3,IA)=GAM(4,IA)*FA/FB
      A=25.
      FA=1.-(R/A)*ATAN(A/R)
      GAM(5,IA)=GAM(4,IA)*FA/FB
      A=30.
      FA=1.-(R/A)*ATAN(A/R)
      GAM(6,IA)=GAM(4,IA)*FA/FB
      WRITE(*,'(F6.1,6F6.0)')R,(GAM(I,IA),I=1,6)
100   CONTINUE
C
      R2=SQRT(2.)
C
1     WRITE(*,111)
111   FORMAT(' ENTER VALUE OF f',$)
      READ(*,112)F
112   FORMAT(F10.3)
      OPEN(6,FILE='LPT1')
      WRITE(6,113)SPAN
113   FORMAT('1FOLLOWING WINGSPAN =',5(F5.0,5X))
C
      DO 1000 IA=1,10
      WRITE(6,115)AC(IA),F
115   FORMAT(/' GENERATING AIRCRAFT = ',A6,8X,'f = ',F5.2)
      DO 900 IT=1,5
      T=TIM(IT)
      DO 800 IS=1,6
      SS=SSPAN(IS)
      GT=SS*F*10.
      T1=T*SQRT(GT/GAM(IS,IA))
      SG=SIG(IS,IA)
      Z=(T1-3.*SG)/R2/SG
      CALL ERF(Z,ERFO)
      PR(IS)=0.5*ERFO
c      ave circ distribution
      sigam=0.2*gam(is,ia)*r2
      z=(gt-gam(is,ia))/sigam
      CALL ERF(Z,ERFO)
      PR(IS)=0.5*ERFO*pr(is)
```

```
800   CONTINUE
      WRITE(6,888)T,PR
888   FORMAT(' TIME=',F5.0,' PR=',6e10.3)
900   CONTINUE
1000  CONTINUE
      GO TO 1
      END


C     ERF.FOR
C
C     ERROR FUNCTION FROM ABRAMOWITZ AND STERGUN
C
C     P,T,A(I)  ERROR FUNCTION CORRELATION COEFF
C
C     RIV   INDEPENDENT VARIABLE
C     RDV   DEPENDENT VARIABLE return 1-erf
C
      SUBROUTINE ERF(Z,RDV)
      DIMENSION A(3)
      DATA P/0.47047/,A/0.3480242,-0.0958798,0.7478556/
C
      IF(Z.LT.0.) THEN
            RIV=-Z
      ELSE
            RIV=Z
      ENDIF
      T=1.0/(1.0+P*RIV)
      ESUM=0.0
      DO 10 I=1,3
10    ESUM=ESUM+A(I)*(T**I)
C
      RDV=ESUM*EXP(-(RIV**2))
      IF(Z.LT.0.) RDV=2.-RDV
C
      RETURN
      END
```

APPENDIX E - ALTERNATIVE SEPARATION MODEL SOFTWARE

The software listings below implement the current version of the alternative separation model. The following changes were made from the separation model in Appendix D:

1)   The average circulations are calculated for 5-10 and 10-20 meters radius (DO 200).

2)   The 10-20-meter average circulation value is used in the probability calculations (JS=2).

3)   The σ value for 20-meter average circulation decay is used in the probability calculations (JD=3).

```
C   HAZPRO1.FOR
C
C   CALCULATES THE WAKE-VORTEX HAZARD PROBABILITY FOR
C   FOLLOWING AIRCRAFT OF WINGSPANS 10,20,30,40,50,60 M.
C   FOR VARIOUS GENERATING AIRCRAFT
C        Uses circulation in place of average circulation
C
      DIMENSION AC(10),SSPAN(6),SPAN(6),SIG(6,10),GAM(6,10)
      DIMENSION PR(6),TIM(5),RC(10)
      CHARACTER*6 AC
      DATA AC/'DC-9','B-737','B-727','B-707','DC-8','DC-8H'
     A,'B-707H','DC-10','L-1011','B-747'/
      DATA SIG/13.0,12.8,12.2,11.4,11.4,11.4
     A,14.5,13.4,12.8,12.6,12.6,12.6
     A,12.4,12.0,11.4,11.3,11.3,11.3
     B,12.6,12.4,11.9,12.1,12.1,12.1
     B,12.6,12.3,12.2,12.2,12.2,12.2
     C,10.7,11.0,11.3,11.5,11.5,11.5
     C,14.6,13.4,13.5,13.2,13.2,13.2
     D,16.7,14.2,13.2,13.1,13.1,13.1
     D,15.0,14.7,14.0,14.0,14.0,14.0
     E,13.8,12.8,12.4,12.4,12.4,12.4/
      DATA GAM/51.,93.,0.,136.,0.,0.
     A,47.,94.,0.,138.,0.,0.
     A,60.,115.,0.,169.,0.,0.
     B,79.,136.,0.,188.,0.,0.
     B,85.,151.,0.,213.,0.,0.
     C,84.,152.,0.,210.,0.,0.
     C,83.,148.,0.,193.,0.,0.
     D,61.,138.,0.,218.,0.,0.
     D,69.,147.,0.,227.,0.,0.
     E,87.,181.,0.,299.,0.,0./
      DATA SSPAN,SPAN/5.,10.,15.,20.,25.,30.,10.,20.,30.,40.,50.,60./
      DATA TIM/67.,80.,107.,144.,160./
        DATA RC/4.8,4.8,4.8,4.0,4.2
```

```
      A,4.0,3.2,5.8,5.5,6.3/
C
      DO 100 IA=1,10
C       USE 20-METER AVERAGE CIRC AS REFERENCE TO GET 15,25,30 METER
VALUES
      B=20.
      R=RC(IA)
      FB=1.-(R/B)*ATAN(B/R)
      A=15.
      FA=1.-(R/A)*ATAN(A/R)
      GAM(3,IA)=GAM(4,IA)*FA/FB
      A=25.
      FA=1.-(R/A)*ATAN(A/R)
      GAM(5,IA)=GAM(4,IA)*FA/FB
      A=30.
      FA=1.-(R/A)*ATAN(A/R)
      GAM(6,IA)=GAM(4,IA)*FA/FB
      WRITE(*,99)AC(IA),R,(GAM(I,IA),I=1,6)
99    FORMAT(1X,A6,F6.1,6F6.0)
100   CONTINUE
C
      DO 200 IA=1,10
C     USE 5-METER, 10-METER AVERAGE CIRC TO GET 5-10 m average circ
      GAM(1,IA)=(GAM(2,IA)*10.-GAM(1,IA)*5.)/5.
C     USE 10-METER, 20-METER AVERAGE CIRC TO GET 10-20 m average circ
      GAM(2,IA)=(GAM(4,IA)*20.-GAM(2,IA)*10.)/10.
      WRITE(*,199)AC(IA),(GAM(I,IA),I=1,2)
199   FORMAT(1X,A6,6F6.0)
200   CONTINUE
      R2=SQRT(2.)
C
1     WRITE(*,111)
111   FORMAT(' ENTER VALUE OF f',$)
      READ(*,112)F
112   FORMAT(F10.3)
      OPEN(6,FILE='LPT1')
      WRITE(6,113)SPAN
113   FORMAT('1FOLLOWING WINGSPAN =',5(F5.0,5X))
C
      JS=2
      JD=3
      DO 1000 IA=1,10
      WRITE(6,115)AC(IA),F,JS,JD
115   FORMAT(/' GENERATING AIRCRAFT = ',A6,8X,'f = ',F5.2
     A,'  JS,JD=',2I2)
```

```
      DO 900 IT=1,5
      T=TIM(IT)
      DO 800 IS=1,6
      SS=SSPAN(IS)
      GT=SS*F*10.
      T1=T*SQRT(GT/GAM(JS,IA))
      SG=SIG(JD,IA)
      Z=(T1-3.*SG)/R2/SG
      CALL ERF(Z,ERFO)
      PR(IS)=0.5*ERFO
c        ave circ distribution
         sigam=0.2*gam(JS,ia)*r2
         z=(gt-gam(JS,ia))/sigam
      CALL ERF(Z,ERFO)
      PR(IS)=0.5*ERFO*pr(is)
800   CONTINUE
      WRITE(6,888)T,PR
888   FORMAT(' TIME=',F5.0,'  PR=',6e10.3)
900   CONTINUE
1000  CONTINUE
      GO TO 1
      END
```

REFERENCES

1. Burnham, D.C. and Hallock, J.N., "Chicago Monostatic Acoustic Vortex Sensing System, Volume IV: Wake Vortex Decay," Report No. FAA-RD-79-103,IV, July 1982, DOT Transportation Systems Center, Cambridge MA. (Please note interchange of Figures 21 and 22 in this report and reversed vortex labels on Figure 40.)

2. Burnham, D.C. and Hallock, J.N., "Chicago Monostatic Vortex Sensing System, Volume II: Decay of B-707 and DC-8 Vortices," Report DOT/FAA/RD-79-103,II, September 1981, DOT Transportation Systems Center, Cambridge, MA.

3. Burnham, D.C. and Hallock, J.N., "Chicago Monostatic Vortex Sensing System, Volume III: Executive Summary: Decay of B-707 and DC-8 Vortices," Report DOT/FAA/RD-79-103,III, January 1982, DOT Transportation Systems Center, Cambridge, MA.

4. Yarmus, J., Burnham, D., Wright, A., and Talbot, T., "Aircraft Wake Vortex Takeoff Tests at O'Hare International Airport," Report DOT/FAA/RD-94-25, August 1994, DOT Volpe National Transportation Systems Center, Cambridge, MA.

5. Burnham, D.C., "How to Use Wake Vortex Measurements to Set Separation Standards," Report No. DOT/FAA/SD-92/1.2, *Proceedings of the Aircraft Wake Vortices Conference - Vol. 2*, October 1991, pp 53-(1-11).

6. Rudis, R., Burnham, D. and Janota, P., "Wake Vortex Decay near the Ground under Conditions of Strong Stratification and Wind Shear," AGARD-CP-584 Conference Proceedings, The Characterization & Modification of Wakes from Lifting Vehicles in Fluids, 20-23 May, 1996, pp. 11-(1-10).

7. Rudis, R.P. and Burnham, D.C., "Comparison of Sodar and Lidar Measurements of Aircraft Wake Vortices," Preprint for ISARS'96 Conference, Moscow, Russia, May 1996.

8. Burnham, D.C., "Analysis of UK Encounters 1982-1990," AGARD-CP-584 Conference Proceedings, The Characterization & Modification of Wakes from Lifting Vehicles in Fluids, 20-23 May, 1996, pp. 21-(1-4).

9. Hallock, J.N., "Vortex Advisory System Safety Analysis, Volume I: Analytical Model," Report No. FAA-RD-78-68,I, September 1978, DOT Transportation Systems Center, Cambridge MA.

10. Critchley, J.B. and Foot, P.B., "United Kingdom Civil Aviation Authority Wake Vortex Database: Analysis of Incidents Reported Between 1982 and 1990," CAA Paper 91015, August 1991.

11. Critchley, J.B. and Foot, P.B., "UK CAA Vortex Database: Analysis of Incidents Reported Between 1972-1990," Report No. DOD/FAA/SD-92/1.1, *Proceedings of the Aircraft Wake Vortices Conference - Vol. 1*, October 1991, pp 8-(1-18).

12. Rossow, V.J. and Tinling, B.E.,"Research on Aircraft/Vortex-Wake Interactions to Determine Acceptable Level of Wake Intensity," *Journal of Aircraft*, Vol. 25, No. 6, June 1988, pp. 481-492.

13. Greene, George C., "An Approximate Model of Vortex Decay in the Atmosphere," *Journal of Aircraft*, Vol. 23, No. 7, July 1986, pp. 566-573.

14. Burnham, D.C., "Chicago Monostatic Vortex Sensing System, Volume I: Data Collection and Reduction," Report DOT/FAA/RD-79-103, I, October 1979, DOT Transportation Systems Center, Cambridge, MA.

15. Hallock, J.N. and Burnham, D.C., "Decay Characteristics of Wake Vortices from Jet Transport Aircraft," AIAA Paper 97-0060, 35th Aerospace Sciences Meeting, January 6-10, 1997, Reno, NV.

16. Vicroy, D.D. and Nguyen, T., "A Numerical Simulation Study to Develop an Acceptable Wake Encounter Boundary for a B737-100 Airplane," AIAA-96-3372, AIAA Atmospheric Flight Mechanics Conference, July 29-31, 1996, San Diego, CA.

17. Abramson, S. and Burnham, D.C., "Ground-Based Anemometer Measurements of Wake Vortices from Landing Aircraft at Airports," AGARD-CP-584 Conference Proceedings, The Characterization & Modification of Wakes from Lifting Vehicles in Fluids, 20-23 May, 1996, pp. 13-(1-7).

18. Burnham, D.C., Hallock, J.N., Tombach, I.H., Brashears, M.R. and Barber, M.R., "Ground-Based Measurements of the Wake Vortex Characteristics of a B-747 Aircraft in Various Configurations," Report No. FAA-RD-78-146, December 1978, DOT Transportation Systems Center, Cambridge, MA.

19. Sherratt, S.R., "Re-Classification of Wake Vortex Wake Groups; a Controller's View," Report No. DOT/FAA/SD/92/1.1, *Proceedings of the Aircraft Wake Vortices Conference - Vol. 1*, October 1991, pp 25-(1-7).

20. Burnham, D.C., "B-747 Vortex Alleviation Flight Tests: Ground-Based Sensor Measurements," Report No. DOT-FAA-RD-81-99, February 1982, DOT Transportation Systems Center, Cambridge, MA.

21. Sullivan, T.E., Hallock, J.N., Winston, B.P., McWilliams, I.G. and Burnham, D.C., "Aircraft Wake Vortex Takeoff Tests at Toronto International Airport," Report No. FAA-RD-78-143, February 1979, DOT Transportation Systems Center, Cambridge MA.

22. Margason, R.J. and Lamar, J.E., "Vortex-Lattice FORTRAN Program for Estimating Aerodynamic Characteristics of Complex Planforms," NASA TN D-6142, Feb. 1971.

23. Sammonds, R.I., Stinnett, Jr., G.W., and Larsen, W.E., "Criteria Relating Wake Vortex Encounter Hazard to Aircraft Response," *Journal of Aircraft*, Vol. 14, No. 10, Oct. 1977, pp. 981-987.

24. Sammonds, R.I., Stinnett, Jr., G.W., and Larsen, W.E., "Wake Vortex Encounter Hazard Criteria for Two Aircraft Classes," Report No. FAA-RD-75-206, June 1976, NASA Ames Research Center, Moffett Field, CA.

25. Holbrook, G.T., "Vortex Wake Hazard Analysis Including the Effect of the Encountering Wing on the Vortex," M.S. Thesis, George Washington University, August 1985.